Redox-sensitive, cholesterol-bearing PEGylated poly(propyleneimine)-based dendrimersomes for drug and gene delivery to cancer cells

*Partha Laskar [†], Sukrut Somani [†], Najla Altwaijry [†], Margaret Mullin [&], Deborah Bowering [‡], Monika Warzecha [†#], Patricia Keating[‡], Rothwelle J. Tate[†], Hing Y. Leung [§], Christine Dufès [†] **

[†] Strathclyde Institute of Pharmacy and Biomedical Sciences, University of Strathclyde, 161 Cathedral Street, Glasgow G4 0RE, United Kingdom

[&] College of Medical, Veterinary and Life Sciences, University of Glasgow, Glasgow G12 8QQ, United Kingdom

[‡] Department of Pure and Applied Chemistry, University of Strathclyde, 295 Cathedral Street, Glasgow G1 1XL, United Kingdom

CMAC Future Manufacturing Research Hub, Technology and Innovation Centre, University of Strathclyde, 99 George Street, Glasgow G1 1RD, United Kingdom

[§] Cancer Research UK Beatson Institute, Garscube Estate, Switchback Road, Bearsden, Glasgow, G61 1BD, United Kingdom

KEYWORDS

Dendrimer, polyethylene glycol, cholesterol, redox sensitivity, gene delivery, drug delivery

ABSTRACT

Stimuli-responsive nanocarriers have attracted increasing attention for drug and gene delivery in cancer therapy. The present study reports the development of redox-sensitive dendrimersomes made of disulphide-linked cholesterol-bearing PEGylated dendrimers, that can be used as drug and gene delivery systems. Two disulphide-linked cholesterol-bearing PEGylated generation 3-diaminobutyric polypropylenimine dendrimers have been successfully synthesized through *in situ* two-step reaction. They were able to spontaneously self-assemble into stable, cationic, nanosized vesicles (or dendrimersomes), with lower critical aggregation concentration values for high cholesterol-bearing vesicles. These dendrimersomes were able to entrap both hydrophilic and hydrophobic dyes, and also showed a redox-responsive sustained release of the entrapped guests in presence of a glutathione concentration similar to that of the cytosolic reducing environment. The high cholesterol-bearing dendrimersome was found to have a higher melting enthalpy, an increased adsorption tendency on mica surface, was able to entrap a larger amount of hydrophobic drug and was more resistant to redox-responsive environment in comparison with its low cholesterol counterpart. In addition, both dendrimersomes were able to condense more than 85% of the DNA at all tested ratios for the low-cholesterol vesicles, and at dendrimer: DNA weight ratios of 1:1 and higher for the high-cholesterol vesicles. These vesicles resulted in an enhanced cellular uptake of DNA, by up to 15-fold compared with naked DNA with the low-cholesterol vesicles. As a result, they increased gene transfection on PC-3 prostate cancer cell line, with the highest transfection being obtained with low-cholesterol vesicle complex at a dendrimer: DNA weight ratio of 5:1 and high-cholesterol vesicle complex at a dendrimer: DNA weight ratio of 10:1. These transfection levels were about 5-fold higher than that observed when

treated with DNA. These cholesterol-bearing PEGylated dendrimer-based vesicles are therefore promising as redox-sensitive drug and gene delivery systems for potential applications in combination cancer therapy.

INTRODUCTION

Despite recent advances in the field of cancer gene therapy, the possibility of using therapeutic genes combined with anti-cancer drugs for cancer treatment is still hampered by the lack of safe delivery systems able to carry both therapeutic DNA and drug simultaneously and to selectively deliver them to the tumors, without secondary effects to healthy tissues. [1] The synthesis of novel "smart" delivery systems able to overcome these issues is therefore urgently needed. In order to remediate this issue, we propose to conjugate cholesterol and PEG to the surface of generation 3-diaminobutyric polypropylenimine (DAB) dendrimer, with a redox-sensitive disulphide linkage, and evaluate the potential use of this novel dendrimer as a drug and gene delivery system.

Cationic dendrimers are emerging as potential non-viral vectors for delivering nucleic acids and anti-cancer drugs to cancer cells. These polymers are highly branched, three-dimensional macromolecules with modifiable surface functionalities that have been largely exploited to achieve the conjugation of targeting moieties and the binding of drugs or nucleic acids for therapeutic applications. Furthermore, their constitutive dendrons delimitate internal cavities, that can be used for the encapsulation of various chemically sensitive drugs. Their high aqueous solubility, low toxicity, compact globular shape made them ideal carriers for anti-cancer drugs. [2] Dendrimers can also facilitate the passive targeting of anti-cancer drugs to tumor tissue. This selective accumulation of macromolecules in tumors, termed "enhanced permeability and retention (EPR) effect", is the consequence of the combination of reduced lymphatic drainage and increased permeability of tumor vasculature to macromolecules. [3] Positively charged dendrimers can form stable ionic complexes with negatively charged plasmid DNA, but also bind easily to the negatively charged cell surface through electrostatic interactions, leading to their cellular internalization by endocytosis. [4-6]

In this work, we have chosen to use generation 3-diaminobutyric polypropylenimine (DAB) dendrimer, as it has been reported to be more efficacious than its higher generations for gene transfection. [7] In addition, we recently demonstrated that tumor-targeted generation 3-DAB dendrimer complexed to therapeutic plasmid DNA led to successful gene expression and therapeutic efficacy in mice bearing subcutaneous tumors following intravenous injection. [8-12]

Recently, the development of various self-assembled nanostructures (such as micelles, vesicles or dendrimersomes) based on surface-modified amphiphilic dendrimers following conjugation with diverse hydrophobic groups (such as aromatic, long hydrophobic chains, fluorinated groups) has shown promises for further biomedical applications. [13-15] Since the hydrophobic interactions are one of the main driving forces for any aggregated structure, the conjugation of lipidic alkyl chains to dendrimers would not only increase the hydrophobicity of the dendrimers and facilitate their self-assembly, but would also make them form more compact and smaller sized dendriplexes. [16-17] Based on this, we have chosen to conjugate DAB dendrimer with a more lipophilic moiety, cholesterol, which is an essential structural and functional constituent of animal cell membrane. Due to its higher hydrophobicity compared with the hydrocarbon chains of fatty acids, cholesterol has been previously used for the synthesis of polymer- and surfactant-based self-assembled nanostructures. [18-20] Cholesterol enhances the stability of the hydrophobic rigid microenvironment of nanostructures, helps drug delivery systems to cross the cellular membrane more easily, and also increases the transfection efficacy of cholesterol-based gene vectors in various cell lines due to its strong fusogenic activity. [21]

Poly(ethylene glycol) (PEG) will also be conjugated to the cholesterol-bearing DAB-dendrimer as this stealth material was previously reported to increase the water solubility and to reduce non-specific interactions with circulatory proteins, thus leading to an enhanced

circulatory life time of drug and gene delivery systems. [22-25] We recently demonstrated that the conjugation of low molecular weight PEG (2 kDa) to generation 3- and generation 4-DAB dendrimers significantly decreased their cytotoxicity on B16F10-Luc cells, by more than 3.4-fold compared to unmodified dendrimers. [26] In addition, these PEGylated dendrimers complexed to DNA at dendrimer: DNA ratios of 20:1 and 10:1 were able to increase gene expression on B16F10-Luc, A431, DU145, PC3-Luc cells lines, compared to the unmodified dendriplex.

Stimuli- responsive polymers have gained widespread interest as they are able to undergo structural changes in the presence of an external stimulus such as pH, light or redox. In this regard, amphiphilic dendrimers containing a disulphide linkage in their structural backbone are particularly interesting, as this group can be cleaved into the corresponding thiols in presence of a reducing biothiol, such as glutathione (GSH), triggering the destruction of the delivery systems and the release of the guest at the desired site of action. [27] This is particularly important in cancer therapy, as glutathione is present in abundance in cancer cells: its concentration was found to be different in intracellular (~10 mM) and extracellular (<10 μM) compartments of living cells. It is nearly 4-fold higher than that of normal tissue in cancer cells. [27]

The objectives of this study were therefore 1) to synthesize and characterize disulphide-linked cholesterol-bearing PEGylated amphiphilic DAB dendrimers, 2) to evaluate their self-assembly formation into nanostructures and their ability to entrap drugs, 3) to assess the redox sensitivity of these nanostructures, 4) to evaluate DNA condensation by the dendrimer-based nanostructures and 5) to assess the cell viability, cellular uptake and transfection efficacy of these structures complexed with DNA on prostate cancer cells *in vitro*.

MATERIALS AND METHODS

Materials

Generation 3- diaminobutyric polypropylenimine dendrimer (DAB) was purchased from SyMO-Chem (Eindhoven, The Netherlands). Thiocholesterol (CHOLSH), glutathione (GSH), trimethylamine (TEA), N-Phenyl-1-naphthylamine (NPN), Nile Red, Rhodamine 6G (R6G), trifluoroacetic acid (TFA), the deuterated solvents $CDCl_3$ and D_2O, and a double-sided Biodialyser (sample reservoir size: 1 mL) were obtained from Sigma Aldrich (Poole, UK). Anhydrous tetrahydrofuran (THF), acetonitrile (HPLC grade) and methanol (MeOH) came from Fisher Scientific (Loughborough, UK). Orthopyridyl disulfide (OPSS) polyethylene glycol (PEG) succinimidyl carboxymethyl ester (OPSS-PEG-SCM) was purchased from JenKem Technology (Plano, TX). The expression plasmid encoding β-galactosidase (pCMVsport β-galactosidase) was obtained from Invitrogen (Paisley, UK). It was purified using an Endotoxin-free Giga Plasmid Kit (Qiagen, Hilden, Germany). Quanti-iT® PicoGreen® dsDNA reagent and tissue culture media were purchased from Life Technologies (Paisley, UK). Vectashield® mounting medium containing 4',6-diamidino-2-phenylindole (DAPI) came from Vector Laboratories (Peterborough, UK). Label IT® Fluorescein Nucleic Acid Labeling Kit was obtained from Cambridge Biosciences (Cambridge, UK). Passive lysis buffer was obtained from Promega (Southampton, UK). Bioware® androgen-irresponsive PC-3M-luc-C6 human prostate adenocarcinoma that expresses the firefly luciferase was purchased from Caliper Life Sciences (Hopkinton, MA).

Synthesis and characterization of the disulphide-linked cholesterol-bearing PEGylated dendrimers

Amine-terminated, generation 3-diaminobutyric poly(propyleneimine) dendrimer (DAB) was first conjugated to PEG using OPSS PEG succinimidyl carboxymethyl ester (OPSS-PEG-SCM) and then to thiocholesterol (CHOLSH) through disulphide linkage using MeOH-THF (5:1) as solvent (Scheme 1). Briefly, TEA (20 equivalents, 66.2 µL) was added as a whole to a solution of DAB (1 equivalent, 40 mg) in 1.5 mL MeOH. After 30 minutes of stirring at 20 ºC, a freshly prepared methanolic solution of OPSS-PEG-SCM (0.5 and 1 equivalents, 27.19 mg and 54.39 mg respectively for low- and high-cholesterol dendrimers, in 1.5 mL methanol) was added dropwise to DAB over 10-12 minutes. The reaction mixture was then stirred at 37 ºC for 6 h, protected from light.

Thiocholesterol (0.5 and 1 equivalents (4.77 mg and 9.54 mg) respectively for low-cholesterol and high-cholesterol dendrimers, in 0.6 mL THF) was then added as a whole to the reaction mixture containing PEGylated DAB. The reaction mixture, initially colorless, gradually became yellow, and was left stirring at 37 ºC, protected from light. After 15 h, distilled water (5 mL) was added to the reaction mixture. The water-soluble modified dendrimers were purified by dialysis against distilled water (2 L), changed twice per day for 3 days at 25°C, using dialysis tubing with a molecular weight cut-off of 3.5 kDa, to remove organic solvents and excess M-PEG, before being filtrated with Whatman cellulose filter paper and freeze-dried using a Christ Epsilon 2-4 LSC freeze dryer (Osterode am Harz, Germany). The final product DAB-PEG-SS-CHOL (DPSC), a white colored compound, was stored at 0-4 ºC for long-term storage.

The infrared spectra of low- and high-cholesterol dendrimers, as well as all the starting materials, were obtained using an IRSpirit® QATR-S Fourier Transform infrared (FTIR) spectrophotometer

with attenuated total reflectance (ATR) probe (Shimadzu, Kyoto, Japan). Transmittance (4000–400 cm^{-1}) was recorded at a 4 cm^{-1} resolution, and spectra were processed with the LabSolutions IR® software (Shimadzu, Kyoto, Japan). The ^{1}H-NMR spectra of both low- and high-cholesterol dendrimers (2-3 mg in 0.5 mL deuterated solvents) were recorded on a Bruker Avance® III-HD500 NMR spectrometer (Billerica, MA), using the residual proton resonance of the solvent as the internal standard.

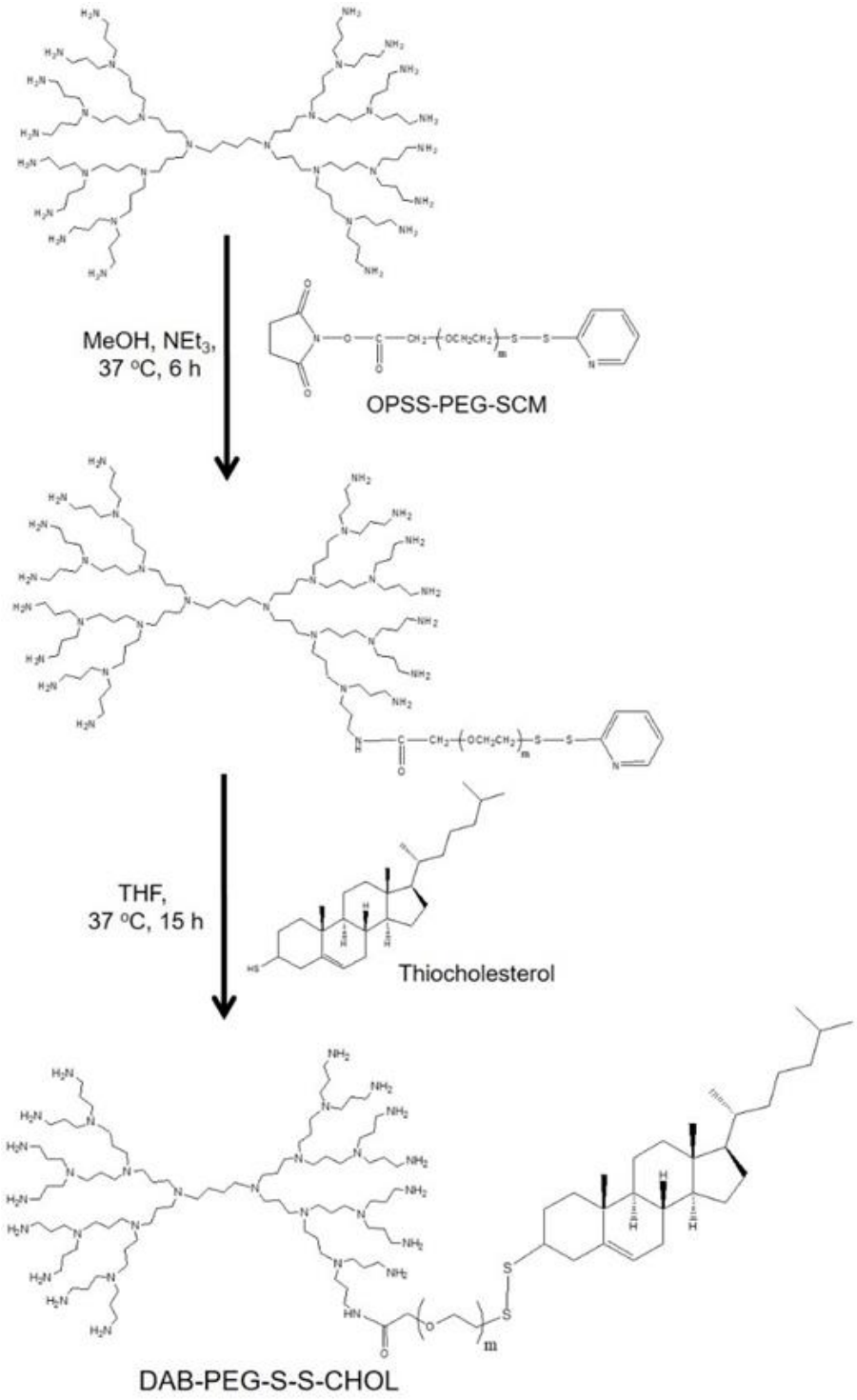

Scheme 1. General synthetic scheme of cholesterol-modified PEGylated dendrimers, with m=45.

The molecular weights of low- and high-cholesterol dendrimers were determined by Matrix-assisted laser desorption ionization time-of-flight (MALDI-TOF) mass spectrometry, using an Axima-CFR® mass spectrometer (Kratos Analytical, Shimadzu, Kyoto, Japan) and α-Cyano-4-hydroxycinnamic acid as the matrix. The matrix was prepared at a concentration of 10 mg/mL in a solvent mixture (acetonitrile/water, 60/40 v/v, with 0.1% TFA). The sample solution (10 µL) was added to the matrix solution (10 µL) in 1/1 (v/v) ratio and thoroughly mixed. One µL of this mixture was then added to the MALDI sample plate and air-dried before measurement. The instrument was operated in a linear mode with a 4 point calibration. A N_2 laser operating at 337 nm was used to generate the ions before being accelerated to 20 kV.

Evaluation of the self-assembly formation of the dendrimers

The ability for low-and high-cholesterol dendrimers to self-assemble was assessed using a steady-state fluorescence technique with N-Phenyl-1-naphthylamine (NPN) as fluorescence probe molecule. To this end, 0.75 µL NPN stock solution (1.32×10^{-3} M, 2.89 mg in 10 mL methanol) were added to 5-mL plastic vials. Following complete evaporation of the solvent after 5-6 h, 1 mL low- and high-cholesterol dendrimer solutions prepared at concentrations ranging from 1 to 400 µg/mL in PBS (pH 7.4), was added to the vials, making the final probe concentration 1×10^{-6} M. Each sample was vigorously vortexed for 5 minutes and then incubated for 16 h at 20 ºC, protected from light, before measurement. Fluorescence spectra of NPN were then recorded with a Varian Cary Eclipse Fluorescence spectrophotometer (Palo Alto, CA) (λ_{exc}: 340 nm, λ_{em}: 360-600 nm, excitation and emission slit at 5 nm and 10 nm respectively).

Hydrodynamic size and zeta potential of dendrimer self-assembled nanostructures

The hydrodynamic diameter (d_H) and zeta potential of dendrimer self-assembled nanostructures in aqueous medium (PBS, pH 7.4) at 37 ºC were measured at concentrations ranging from 50 to 400 µg/mL (over CAC value) by dynamic light scattering (DLS) using a Malvern Nano ZS instrument (Malvern Instruments, Malvern, UK). A 4 mW He-Ne laser (λ = 632.8 nm) was used as a source and scattering photons were collected at 173º scattering angle.

Formation of low-and high-cholesterol dendrimer-based vesicles

Observation of the morphology of the self-assembled nanostructures

The morphology of the low-cholesterol and high-cholesterol dendrimer-based nanostructures (400 µg/mL in PBS pH 7.4) was observed by transmission electron microscopy, using a JEOL JEM-1200EX transmission electron microscope (Jeol, Tokyo, Japan) operating at an accelerating voltage of 80 kV. Three µL of each sample in PBS (pH 7.4) was drop cast on a carbon-coated copper grid (400 mesh size) and was kept in desiccators overnight for drying before imaging.

Encapsulation of hydrophilic dye R6G by the self-assembled nanostructures

R6G solution (1.02×10^{-2} M, 4.89 mg/mL in methanol, 28.18 µL and 19.85 µL) was respectively added to 1.15 mg of low-cholesterol and 0.81 mg of high-cholesterol dendrimers. Following evaporation of methanol by a stream of N_2 gas, the mixture of dendrimers with R6G was soaked in 1 mL PBS buffer pH 7.4 for 3 h (until the dispersion became homogeneous) and vortexed for 10 min. PBS buffer (pH 7.4) was then added to obtain a final dendrimer solution with a concentration of 400 µg dendrimer per mL and 47 µg R6G per mL (1×10^{-4} M). The dendrimer

solution containing R6G was vortexed for 2 min and incubated for 20 h at 25 ºC to allow encapsulation of the hydrophilic dye. To remove the unencapsulated dye, the dendrimer solution (1 mL) was dialyzed in a double-sided Biodialyzer cell using a dialysis membrane with a molecular weight cut-off of 2000 Da, against 60 mL PBS buffer (pH 7.4) for 24 h with 4 changes of the buffer. The dialyzed solution was kept protected from light and its fluorescence was quantified by spectrofluorimetry (λ_{ex}: 480 nm, λ_{em}: 500-700 nm), using a Varian Cary Eclipse spectrofluorometer (Agilent Technologies, Santa Clara, CA).

Thermal analysis of phase transition behavior of low-and high-cholesterol dendrimer-based vesicles

Transmittance of low-cholesterol and high-cholesterol dendrimer-based vesicles (400 µg/mL in PBS buffer pH 7.4) was measured at temperatures ranging from 20 ºC to 90 ºC, using a Varian Model-Cary 5000 spectrophotometer (Agilent Technologies, Santa Clara, CA), with a Cary automated temperature controller UV0904M400 (Agilent Technologies, Santa Clara, CA), to measure the cloud point. Differential scanning calorimetry (DSC) measurements for low-cholesterol and high-cholesterol dendrimer-based vesicles (2 mg/mL in PBS pH 7.4) were done using a Netzsch DSC214 Polyma differential scanning calorimeter (Netzsch-Gerätebau GmbH, Selb, Germany) to measure the phase transition behavior of the vesicles. To this end, 3.1 ± 0.1 mg of sample was transferred to a 40 µL aluminium pan by micropipetting. Pans were hermetically sealed with aluminium lids. Blank and reference pans were prepared with 3.1 ± 0.1 mg of PBS solution. Samples were cooled to -15°C at a rate of 2 °C/min and held for 5 min at -15°C prior to heating at a rate of 2 °C/min. A repeat cycle was carried out on each sample. Blank correction was carried out with the PBS solution under the same measurement conditions prior to

sample analysis. Analysis of the results was carried out with Netzsch Proteus Analysis Software v7.0.1 (Netzsch-Gerätebau GmbH, Selb, Germany), with onset temperature, peak temperature and enthalpy of measured peaks determined.

Atomic force microscopy (AFM) imaging of dendrimer-based vesicles

Low-cholesterol and high-cholesterol dendrimer-based vesicles were visualized by atomic force microscopy (AFM) to assess their size and shape. Data were collected by a Dimension Icon® AFM (Bruker, Santa Barbara, CA) using a PeakForce Tapping® scanning mode at 20 ºC with a ScanAsyst-Air® probe (Bruker, Santa Barbara, CA) with nominal spring constant k =0.4 N/m and nominal tip radius of 2 nm. One drop (10 µL) of dendrimer solution (400 µg/mL in PBS pH 7.4) was placed on a freshly cleaved mica surface and was left to dry at 20 ºC overnight, protected from light, before measurements. All images were analyzed using NanoScope Analysis 1.5 software (Bruker, Santa Barbara, CA). Height images were corrected by first order flattening.

Evaluation of redox sensitivity of the dendrimer-based vesicles

Size measurement

The hydrodynamic diameter was measured at different time intervals by dynamic light scattering as described above for low- and high-cholesterol dendrimer-based vesicles (1.5 mL, 100 µg/mL in PBS pH 7.4), incubated with or without glutathione (10 µm and 10 mM) at 37 ºC. Sample solutions in presence and absence of glutathione were prepared by mixing 75 µL of stock dendrimer solutions (2 mg/mL) with 150 µL glutathione solution (100 mM or 100 µM) and 1275 µL PBS (pH 7.4), or 1425 µL PBS solution (pH 7.4) for control measurement. The samples were then incubated in the dark under stirring at 37 ºC for 48 h.

Redox-sensitive release of Nile Red from the vesicles

The redox-triggered release of an entrapped lipophilic dye, Nile Red, from the low- and high-cholesterol dendrimer-based vesicles was assessed using the reducing agent glutathione.

In order to entrap Nile Red into the vesicles, low- and high-cholesterol dendrimer-based vesicles (2 mg/mL) were prepared in PBS (pH 7.4) and equilibrated for 24h at 20 ºC. Nile Red solution (40 µL, 5 mg/mL in methanol) was added into an empty plastic vial and the methanol was evaporated by a stream of N_2 gas. Then, 1 mL of stock dendrimer-based vesicles was added to the vial containing Nile Red and the mixed dispersion was stirred at 20 ºC for 40 h, protected from light. The dispersions were then filtered through hydrophilic cellulose acetate membranes with pore size of 0.45 µm to remove free Nile Red.

To test the glutathione-sensitive release of entrapped Nile Red from the vesicles, 75 µL of Nile Red-entrapped vesicles (2 mg/mL) were mixed with either 1425 µL PBS for control measurement, or 150 µL glutathione solutions (100 mM or 100 µM) and 1275 µL PBS to get the experimental concentration in absence and presence of glutathione. Fluorescence spectra of Nile Red were recorded (λ_{ex}: 540 nm, λ_{em}: 560-800 nm, excitation and emission slits at 10 nm and 20 nm respectively) at different time intervals, considering the addition of glutathione solution as the start of the experiment.

Characterization of dendriplex formation

Evaluation of DNA condensation

The ability of cholesterol-bearing dendrimers to complex negatively charged plasmid DNA encoding β-galactosidase was evaluated by a PicoGreen® assay, performed according to the

supplier's protocol. On the day of the experiment, PicoGreen® reagent was diluted 200-fold in Tris–EDTA (TE) buffer (10 mM Tris, 1 mM EDTA, pH 7.5). DNA solution (500 µL, 10 µg/mL in TE buffer) was added to each sample of dendrimer solution (500 µL in TE buffer) and vortexed to prepare 1 mL of dendrimer: DNA complexes, with dendrimer: DNA weight ratios of 20:1, 10:1, 5:1, 2:1, 1:1, 0.5:1 and 0:1. One mL PicoGreen® solution was then added to the dendriplexes and vortexed immediately before the first measurement. The fluorescence intensity of PicoGreen® (λ_{ex}: 480 nm, λ_{em}: 520 nm, excitation and emission slits: 5 nm each) in presence of the dendriplexes was measured at various times using a Varian Cary Eclipse Fluorescence spectrophotometer (Palo Alto, CA). Results were represented as percentage of DNA condensation.

Agarose gel retardation assay was also performed to assess DNA condensation ability of the dendrimers. Dendriplexes were prepared at various dendrimer: DNA weight ratios from 20:1 to 0.5:1, with a constant DNA concentration of 20 µg/mL. After mixing with the loading buffer (2 µL), the samples (10 µL) were loaded on a 1X Tris-Borate-EDTA (TBE) (89 mM Tris base, 89 mM boric acid, 2 mM Na_2-EDTA, pH 8.3) buffered 0.8% (w/v) agarose gel containing ethidium bromide (0.4 µg/mL), with 1x TBE as a running buffer and HyperLadder 1Kb as a DNA size marker. The gel was run at 50 V for 1 h and then photographed under UV light.

Size and zeta potential measurement

Hydrodynamic diameter and zeta potential of dendriplexes was measured by dynamic light scattering (DLS) using a Malvern Nano ZS instrument (Malvern Instruments, Malvern, UK), immediately after mixing a fixed amount of DNA (50 µg) to various dendrimer concentrations in 5% glucose solution (dendrimer: DNA weight ratios: 0.5:1, 1:1, 2:1, 5:1, 10:1 and 20:1).

Observation of the morphology of the dendriplexes

The morphology of the dendriplexes was observed using TEM as described above at an accelerating voltage of 80 kV. Three µL of each dendriplex solution in PBS (pH 7.4) was drop cast on a carbon-coated copper grid (400 mesh size) instantaneously after mixing of a fixed amount of DNA (50 µg) to various dendrimer concentrations (dendrimer: DNA weight ratios: 5:1 and 10:1). The grid was then kept in a desiccator overnight for drying before imaging.

In vitro analysis

Cell culture

Human prostate adenocarcinoma PC3M-Luc cells were grown as monolayers in Minimum Essential Medium (MEM), supplemented with 10% (v/v) fetal bovine serum, 1% (v/v) L-glutamine and 0.5% (v/v) penicillin–streptomycin. Cells were cultured at 37 °C in a 5% carbon dioxide, humid atmosphere.

Evaluation of cell viability

The cell viability of modified dendrimers was evaluated using a standard MTT assay. To this end, PC-3 cells were seeded at a density of 5 000 cells per well in 96-well plates and grown at 37 °C for 24 h in a 5% carbon dioxide, humid atmosphere. They were then treated with different concentrations of dendrimer solution (ranging from 5 to 45 µg/mL) for various incubation time (24, 48 and 72 h). Following treatment, 50 µL of MTT solution (5 mg/mL in PBS pH 7.4) was added in each well and incubated for 4 h at 37 °C. Medium was then removed and 200 µL DMSO was added in each well to solubilize the formazan dye produced during the reduction of

MTT by the living cells. The amount of formazan dye was measured using spectrophotometry at 540 nm with a Multiskan Ascent® plate reader (Thermo Scientific, Waltham, MA).

Cellular uptake of dendriplexes

Qualitative analysis

The cellular uptake of low-and high-cholesterol, dendrimer-based vesicles complexed to DNA was qualitatively assessed using confocal microscopy. Labeling of plasmid DNA with the fluorescent probe fluorescein was performed using a Label IT® Fluorescein Nucleic Acid Labeling kit, as described by the manufacturer. PC-3 cells were seeded on coverslips in 6-well plates at a concentration of 10^5 cells per well and grown for 48 h at 37 °C. The cells were then treated with fluorescein-labelled DNA (2.5 μg/well) complexed to low-and high-cholesterol vesicles, at a dendrimer: DNA weight ratios of 5:1 and 10:1 for 2 hours at 37 °C. Control wells were also prepared with naked DNA or remained untreated. The cells were then washed three times with 3 mL phosphate buffered saline (PBS) before being fixed with 2 mL methanol for 10 min at 20 ºC. They were then washed again with 3 mL PBS. Upon staining of the nuclei with Vectashield® mounting medium containing DAPI, the cells were examined using a Leica TCS SP5 confocal microscope (Wetzlar, Germany). DAPI (which stained the cell nuclei) was excited with the 405 nm laser line (emission bandwidth: 415-491 nm), fluorescein (which labelled the DNA) was excited with the 514 nm laser line (emission bandwidth: 550-620 nm).

Quantitative analysis

Quantification of cellular uptake of the dendrimer-based vesicles complexed to DNA was carried out by flow cytometry. PC-3 cells were seeded at a density of 10^5 cells per well in 6-well plates

and grown at 37 °C for 72 h, before being treated fluorescein-labeled DNA (2.5 µg DNA/well) complexed with the vesicles at dendrimer: DNA weight ratios of 5:1 and 10:1. Other wells were treated with DAB dendriplex and DNA solution as positive and negative controls respectively. After 2 h incubation with the treatments, single cell suspensions were prepared (using 250 µL trypsin per well, followed by 500 µL medium per well once the cells have detached), before being analyzed using a FACSCanto® flow cytometer (BD, Franklin Lakes, NJ). Their mean fluorescence intensity was analyzed with FACSDiva® software (BD, Franklin Lakes, NJ), counting ten thousand cells (gated events) for each sample.

Evaluation of gene expression of the DNA complexed with the dendrimer-based vesicles

The transfection efficacy of the DNA complexed by the dendrimer-based vesicles was assessed using a plasmid DNA encoding β-galactosidase (pCMV β-gal). PC-3 cells were seeded at a concentration of 2 000 cells/well in 96-well plates and left to grow for 72 h at 37 °C in a 5% CO_2 atmosphere. They were then treated with the complex in quintuplicate at various dendrimer: DNA weight ratios (20:1, 10:1, 5:1, 2:1, 1:1 and 0.5:1). Naked DNA was used as a negative control and DAB-DNA (dendrimer: DNA weight ratio 5:1) served as a positive control. DNA concentration (1 µg/mL) was kept constant throughout the experiment. After treatment, the cells were incubated for 24 h, 48 h and 72 h before analysis. They were then lysed with 1X passive lysis buffer (PLB) (50 µL/well) for 20 min at 37 ºC and then tested for β-galactosidase expression. Briefly, 50 µL of the assay buffer (2 mM magnesium chloride, 100 mM mercaptoethanol, 1.33 mg/mL O-nitrophenyl- β-D-galactosidase, 200 mM sodium phosphate buffer, pH 7.3) was added to the cell lysates and incubated for 2 h at 37 ºC. The absorbance of

the samples was subsequently read at 405 nm using a Multiskan Ascent® plate reader (MTX Lab Systems, Brandenton, FL).

Statistical analysis

Results were expressed as means ± standard error of the mean. Statistical significance was assessed by one-way analysis of variance and Tukey multiple comparison post-test (Minitab® software, State College, PE). Differences were considered statistically significant for P values lower than 0.05.

RESULTS AND DISCUSSION

Synthesis and characterization of the disulphide-linked cholesterol-bearing PEGylated dendrimers

The synthesis of low- and high-cholesterol disulphide-linked PEGylated dendrimers was confirmed by FTIR, ^{1}H-NMR and MALDI-TOF MS. Infrared (ATR) spectra of low-and high-cholesterol dendrimers (Figure S1) showed the presence of a new peak at 1645-1646 cm^{-1} (corresponding to an amide bond) and the absence of a peak at 1719-1740 cm^{-1} (corresponding to the succinimidyl carboxymethyl ester group), in comparison with that of the starting materials OPSS-PEG-SCM DAB-G3 and CHOLSH (Figure S2), thus demonstrating the conjugation of PEG to DAB through amide bond formation.

The conjugation of cholesterol and PEG to DAB was also confirmed by ^{1}H-NMR, as follows: ^{1}H-NMR ($CDCl_3$): δ2.39-2.43 ppm, DAB (N-**CH_2**-CH_2-**CH_2**-N) (a); δ2.44-2.46 ppm, DAB (N-**CH_2**-CH_2-CH_2-NH_2) (b); δ3.98 ppm, PEG (NH-CO-**CH_2**-OCH_2CH_2) (c); δ5.35-5.36 ppm, cholesterol (C=**CH**-CH_2) (d); δ0.67 ppm, cholesterol (CH_2C**CH_3**-CH-$CH_2CH_2CCH_3$) (e) (Figure S3).

Molecular weights of both low- and high-cholesterol dendrimers were assigned using MALDI-TOF mass spectrometry (Figure S4). Both mass spectra mainly exhibited singly charged molecular ions $[M]^{+}$ with their fragmented products. The average molecular weight of low-cholesterol PEGylated DAB was 4210 Da, indicating that the ratios of conjugated PEG as well as cholesterol per dendrimer were nearly 1. The average molecular weight of its high-cholesterol counterpart was 6492 Da, demonstrating that these ratios were nearly 2 (Figure S4). MALDI-

TOF mass spectrometry data was analyzed to calculate the percentage of conjugated lipid to dendrimer, which were 9.5% for the low-cholesterol dendrimer and 12.5% for the high-cholesterol dendrimer.

Both low-and high-cholesterol dendrimers showed relatively low % yield (respectively 43% and 33% for low- and high-cholesterol dendrimers).

^{1}H NMR spectrum of high-cholesterol dendrimer in D_2O showed the peaks of DAB and PEG, but no peak for cholesterol (Figure S5), unlike the NMR spectrum of high-cholesterol dendrimer in $CDCl_3$, where peaks for cholesterol were visible (Figure S3B). The absence of the NMR peaks for cholesterol in D_2O and the reappearance of these peaks in $CDCl_3$ demonstrated the amphiphilic nature of the modified dendrimer with a possible self-organization tendency to form self-assembled nano- or microstructure in aqueous medium. [28] The two-step in situ synthetic procedure applied in this study allowed the successful conjugation of PEG and cholesterol on one amine group, which helped to retain more primary amine groups on the surface of the dendrimers and is crucial for the complexation of nucleic acids.

Evaluation of the self-assembly formation of the dendrimers

To study the possible self-assembly of the low-and high-cholesterol PEGylated amphiphilic dendrimers, steady-state fluorescence technique using NPN as probe molecule was used. Being a hydrophobic fluorescent probe, NPN is weakly fluorescent in water, but its fluorescence intensity increases when it is being solubilized in a non-polar medium or within the hydrophobic core of any self-assembled aggregates. [29] The fluorescence intensity of NPN exhibited a gradual rise of

fluorescence with increasing concentrations of dendrimer in PBS (pH 7.4) with a complete blue shift of the λ_{max} (from ~465 nm at a dendrimer concentration of 0 μg/mL to ~420 nm at a dendrimer concentration of 400 μg/mL) (Figure S6), demonstrating the solubilization of the probe in the hydrophobic domain of the self-assembled aggregate formed by these amphiphilic dendrimers. The initial plateau of the curve showed concentration-independent fluorescence intensity for dendrimer concentrations below 10 μg/mL, which reveals that self-association of the dendrimers starts through the inter-chain aggregation above the critical aggregate concentration, without formation of unimer aggregates (Figure 1). The critical aggregation concentration (CAC) values were calculated from the inflection point of the plot of relative fluorescence intensities (I/I_o, where I and I_o are respectively the fluorescence intensities in the presence and absence of dendrimer) of NPN at various dendrimer concentrations (Figure 1). The CAC values decreased by increasing the degree of cholesterol conjugation: the high-cholesterol dendrimer had a comparatively lower CAC value (~10 μg/mL) than that of the low-cholesterol dendrimer (~21 μg/mL). This might be attributed to the overall higher hydrophobe content of the high-cholesterol dendrimer in comparison with the low-cholesterol dendrimer, as the self-assembled aggregate formation occurs mainly through the hydrophobic interaction among the lipid molecules. The CAC values for the low and high cholesterol-modified PEGylated dendrimers were found to be close to that obtained with generation 1-, generation 2- and generation 3-PAMAM dendrimer conjugated to cholesterol at 40% mole ratio of cholesterol/primary amine (12.5 ± 3.2 μg/mL for generation 2-PAMAM-cholesterol, 28.9 ± 4.1 μg/mL for generation 1-PAMAM-cholesterol and 28.7 ± 3.5 μg/mL for generation 3-PAMAM-cholesterol). [30] They were lower than the CMC observed when using generation-3 PAMAM dendrimers conjugated to cholesterol at 6% and 15% mole ratio of cholesterol/primary amine

(respectively 86.6 ± 5.6 μg/mL and 50.2 ± 5.1 μg/mL). [31] These low CMC facilitated the incorporation of the PAMAM-cholesterol in the PEG-stabilized liposome bilayer. In addition, the CAC values for the low- and high-cholesterol dendrimers were found to be well below those of dendrimersomes and glycodendrimersomes prepared from self-assembling amphiphilic Janus dendrimers (typically between 0.5 mg/mL and 1 mg/mL). [32] The CAC values obtained in our experiments were low, indicating the stability of the self-assemblies in dilute conditions, which is a very important parameter for future applications as drug and gene delivery systems.

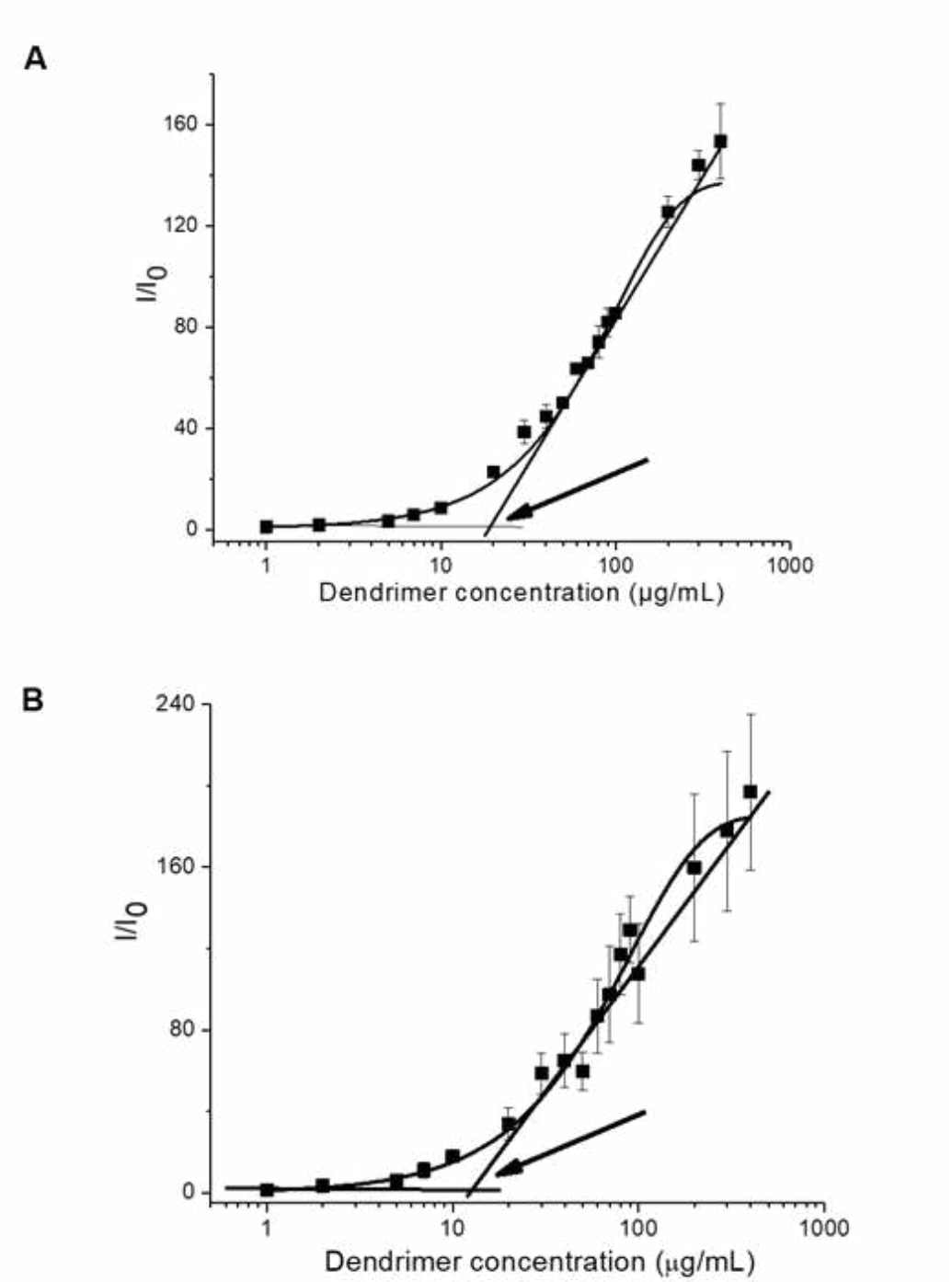

Figure 1. Relative fluorescence intensity (I/I_o) of N-Phenyl-1-naphthylamine in function of the concentration of low-cholesterol dendrimer (A, R^2: 0.99) and high-cholesterol dendrimer (B, R^2: 0.96) in PBS buffer (pH 7.4)

Hydrodynamic size and zeta potential of dendrimer self-assembled nanostructures

Both low-cholesterol and high-cholesterol dendrimer-based self-assembled nanostructures displayed an average size less than 230 nm at all the concentrations tested, with low polydispersity index (PDI) values (respectively 0.25-0.4 and 0.2-0.25 for low and high cholesterol dendrimer-based nanostructures) (Figure 2). Their size gradually decreased from low to high concentrations, to reach their smallest sizes of 91.3 nm ± 11.3 nm and 133.4 nm ± 48.8 nm respectively for low-cholesterol and high-cholesterol dendrimer-based nanostructures. This decrease might be due to the formation of more compact and stable nanostructures at high concentrations, resulting from increased hydrophobic interactions among cholesterol at higher dendrimer concentrations. These sizes were generally lower than those reported for spontaneous or stimuli-sensitive, dendrimer-based vesicular structures made of C17 and C18 alkyl chain-bearing polyamine amphiphilic dendrimers, that ranged from 200 to 500 nm. [33-34] Furthermore, they were below the cut-off size for extravasation, which is 400 nm for most tumors. [35]

Zeta potential experiments demonstrated that these self-assembled nanostructures were bearing a positive zeta potential comprised between 4 mV and 7 mV for both dendrimers. Zeta potential increased with increasing concentrations, to reach maximum values of 5.7 mV ± 0.5 mV and 6.5 mV ± 0.3 mV respectively for low-cholesterol and high-cholesterol dendrimer-based nanostructures. It was similar as that obtained with disulphide cross-linked hyperbranched PAMAM-based vesicles (~5 mV). [36] These positively charged formulations would increase their electrostatic interactions with the negatively charged cellular membranes, resulting in an enhanced cellular uptake of the nanostructures through internalization mechanisms. [37] The modulation of the amount of cholesterol within the dendrimers did not impact on the size and

zeta potential of the low-cholesterol and high-cholesterol dendrimer-based self-assembled nanostructures, that were no statistically different at all measured concentrations.

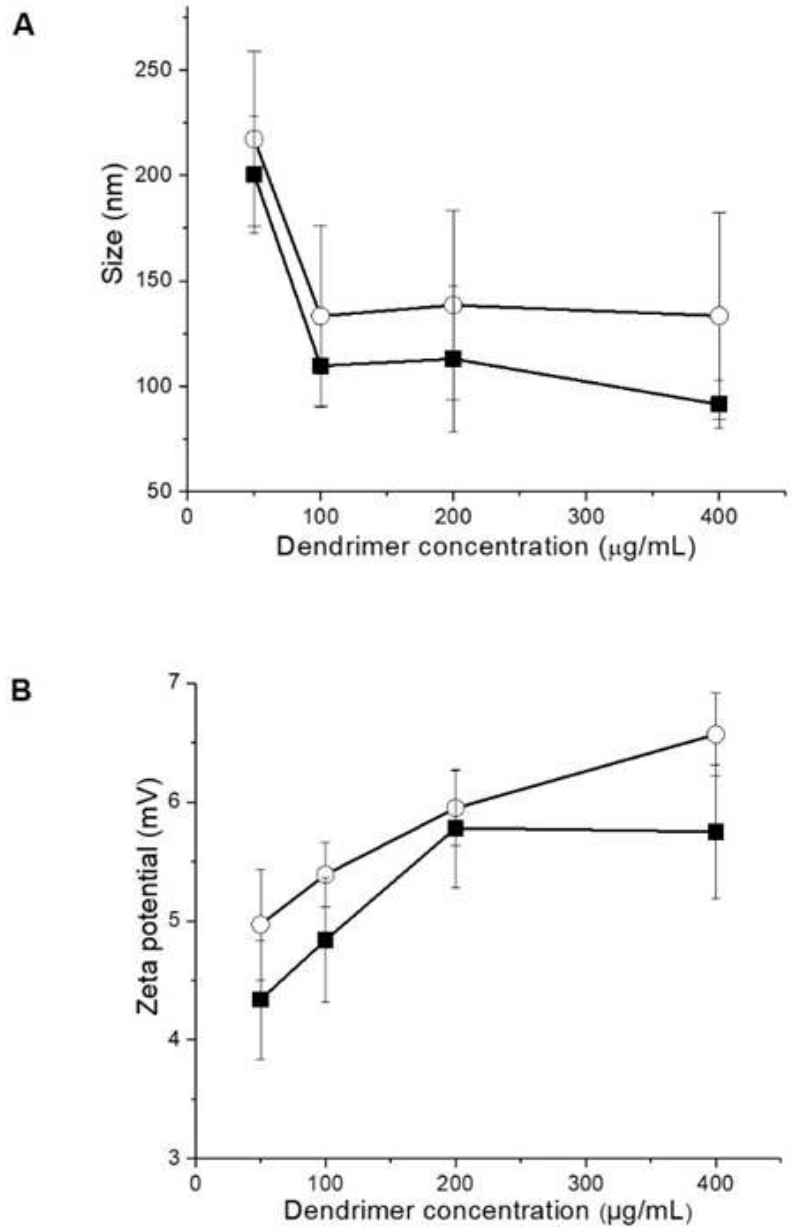

Figure 2. Size (A) and zeta potential (B) of low-cholesterol (■) and high-cholesterol (○) dendrimers self-assembled nanostructures in PBS buffer (pH 7.4) at 37 ºC

Formation of low-and high-cholesterol dendrimer-based vesicles

Observation of the morphology of the self-assembled nanostructures

TEM images of the low-and high-cholesterol dendrimer-based nanostructures revealed the presence of spherical unilamellar vesicles. Their size (lower than 50 nm) was smaller than that observed with DLS, as TEM images were taken following drying of the samples, unlike DLS, where hydrodynamic sizes were being measured.

Encapsulation of hydrophilic dye R6G by the self-assembled nanostructures

Normalized fluorescence spectra of the cationic hydrophilic dye R6G showed the quenching of the fluorescence intensity of the dye in presence of the dendrimer-based vesicles, compared with that of absorbance-matched dye solution (Figure 3). As R6G dye exhibits self-quenching properties, it is possible to investigate whether it is sequestered inside a vesicle-type nanostructure. When a certain amount of hydrophilic dye, R6G is uniformly distributed in water, it fluoresces without any self-quenching effect. However, when some of the dye is being encapsulated within the aqueous core of the dendrimer-based vesicles, the local concentration of the dye within this small-volume core increases, leading to self-quenching. [38] These results therefore demonstrated the encapsulation of R6G in the aqueous core of the dendrimer-based vesicles, with drug loading efficiencies of 0.28 % and 0.20 % respectively for the low-and high-cholesterol dendrimer-based vesicles. This further confirms that the structure of the self-assembly nanostructure is a vesicle, and not a micelle, as a micelle would not be able to entrap hydrophilic dyes.

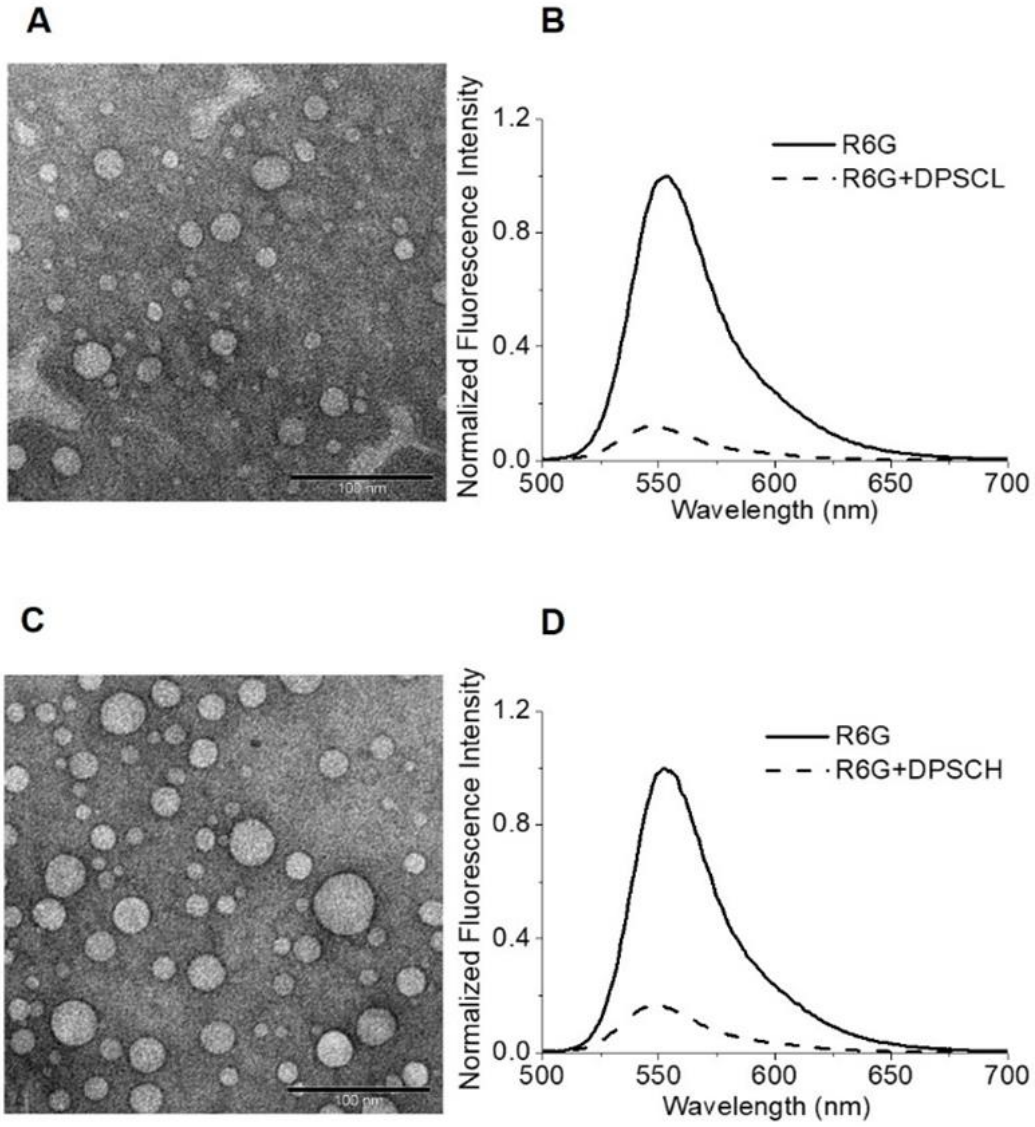

Figure 3. Demonstration of the formation of low- and high-cholesterol dendrimer-based vesicles:

- Unstained TEM images of low-cholesterol (A) and high-cholesterol (C) dendrimer-based vesicles (400 µg/mL in PBS, pH 7.4)

- Normalized fluorescence spectra of R6G in the presence and absence of low-cholesterol (B) and high-cholesterol (D) dendrimer-based vesicles (400 μg/mL in PBS, pH 7.4)

Thermal analysis of phase transition behavior of low-and high-cholesterol dendrimer-based vesicles

Thermal stability at physiological conditions (pH 7.4, 37 ^{o}C) is an important parameter for drug delivery carriers. Percent transmittance (%T) with increasing temperature (Figure S7) showed more than 95% transmittance for both low-cholesterol and high-cholesterol dendrimer-based vesicles (400 μg/mL in PBS buffer pH 7.4), suggesting there was no lower critical solution temperature (LCST) or cloud point (CT) in temperature ranging from 20 to 90 °C. These results demonstrated that there should be no phase separation of dendrimer-based vesicles at body temperature (37 ^{o}C) and therefore no premature release of any entrapped pharmaceutically active agent at body temperature. The cationic nature and PEGylation of both cholesterol-modified amphiphilic dendrimers make them more hydrophilic and stable in water at even higher temperatures at this concentration in comparison with cholesterol-based PEGylated polymers (LCST~57-65 ^{o}C) or high molecular-weight PEGylated biaryl-based amphiphilic dendrons (LCST~31-42 ^{o}C). [18,39]

To investigate the impact of the steroidal lipid molecule on the backbone structure of the PEGylated dendrimers, differential scanning calorimetry was performed. An endothermic melting peak (T_m) was visible at nearly 0 °C (-0.6 °C and -0.8 °C respectively for low-cholesterol and high-cholesterol dendrimer-based vesicles) during the heating phase. It also appeared during the second heating cycle (Figure 4). This melting peak (T_m) of heating is responsible for the phase change of the vesicle membrane, from “gel” state to “liquid crystalline”

or “fluid” state, which is similar to that of another unsaturated lipid-based liposomal formulation, palmitoyl-2-oleoyl-sn-glycero-3-phosphocholine (POPC; T_m= –2 ºC). [40-41] The presence of unsaturation in cholesterol and/or in the disulphide bond might be the reason for such low T_m. Although both dendrimer-based vesicles showed nearly the same melting peak, the melting enthalpy (area under the endothermic melting curve) decreased to a lower value from high-cholesterol to low-cholesterol vesicles (Table S1), due to a progressive ‘‘dilution’’ of the lipids (cholesterol) in the membrane from high-cholesterol to low-cholesterol dendrimer-based vesicles. [41]

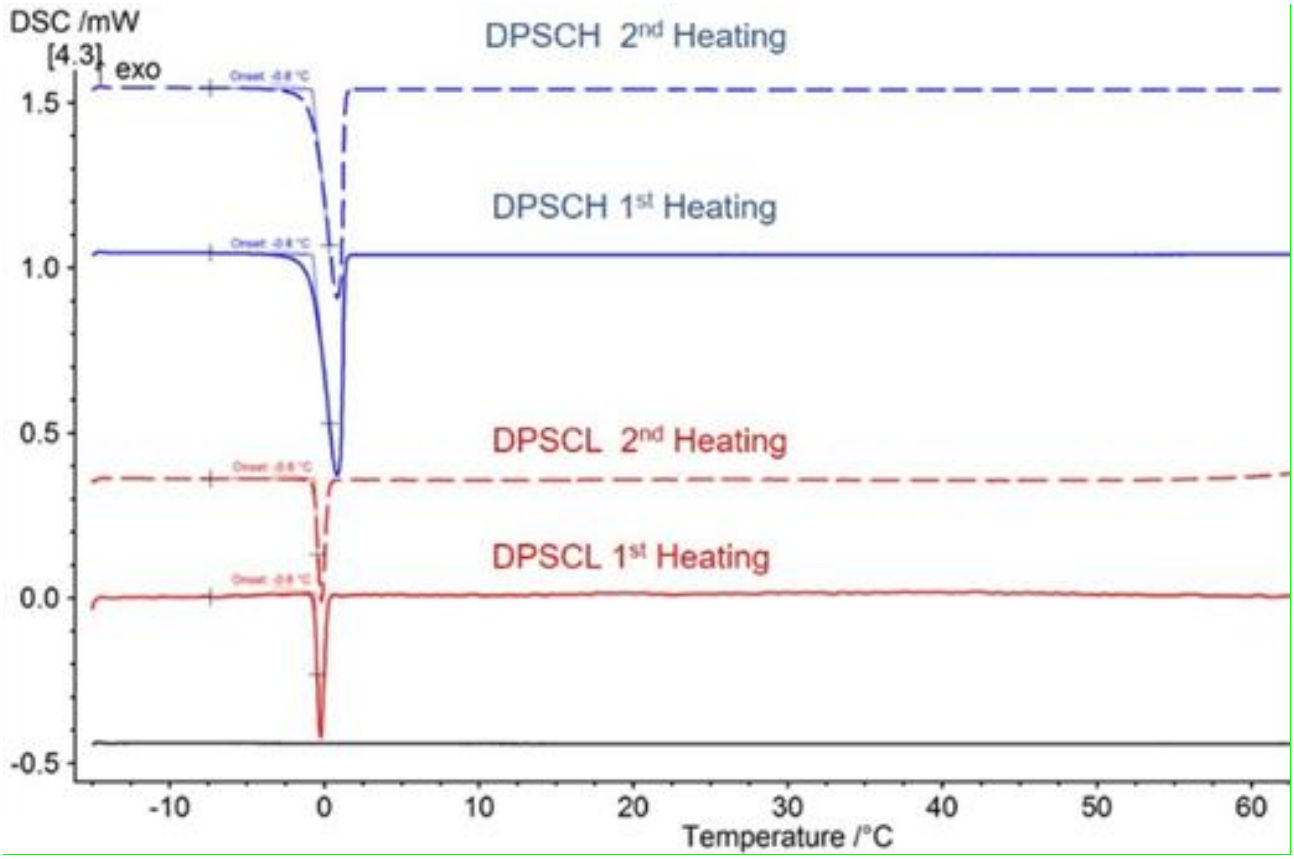

Figure 4. DSC spectra of low-cholesterol (DSPCL, red) and high-cholesterol (DSPCH, blue) dendrimers for the first heating (2 °C.min^{-1}) and second heating cycles (2 °C.min^{-1})

AFM imaging of vesicular aggregates

AFM images were recorded for both dendrimer-based vesicles in PBS (pH 7.4) adsorbed after air drying on freshly cleaved mica surface. Low-cholesterol, dendrimer-based vesicles kept their vesicular structure, but their shape was slightly deformed and changed from spheres to spherical caps, as seen in the cross-section analysis (Figure 5). This was probably due to the strong adsorption of lipid-bearing dendrimer onto the freshly cleaved mica surface, which was also the reason behind the broadening of their diameter. The effect of adsorption of the vesicles onto mica surface was even enhanced in the case of high-cholesterol dendrimer-based vesicles, whose dendrimers contain a larger amount of lipids. This led to a more pronounced deformation of the high-cholesterol vesicles and a wider spreading of these vesicles on the mica surface (Figure 5). [42-43] By comparison, the preparation of TEM carbon grids resulted in a much limited deformation of the vesicles, due to the lower surface energy of these grids, whereas the vesicles were subjected to pronounced deformation when in contact with the mica surface, even leading to fusion, as reported for some liposomes and polymersomes. [42-43] The spherical caps had an average typical height of about 20 nm and 10 nm respectively for low-cholesterol and high-cholesterol dendrimer-based vesicles, which further corroborates the spreading of the high-cholesterol vesicles, producing an almost flat film on the mica surface because of their higher lipid content. [42-43]

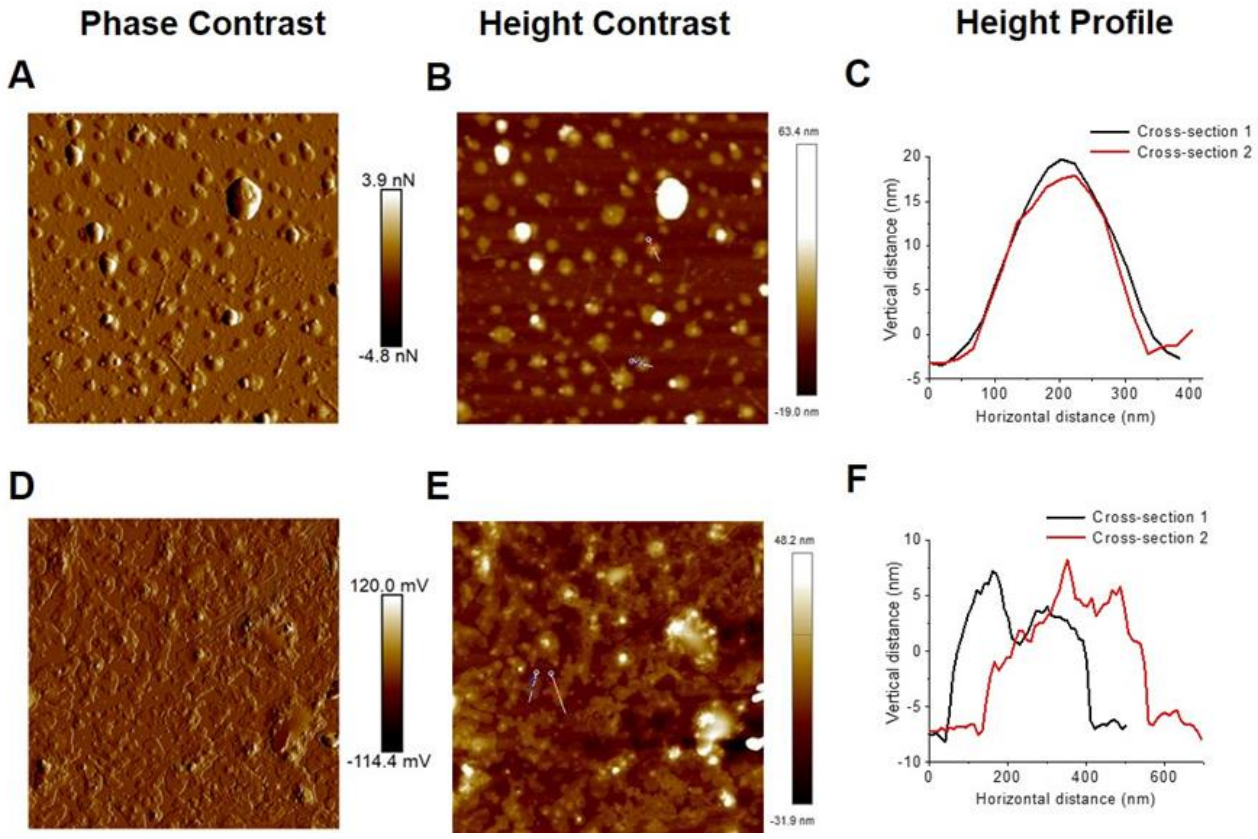

Figure 5 Tapping mode AFM phase and height contrast images of 5 x 5 μm surfaces of low-cholesterol (A, B) and high-cholesterol (D, E) dendrimer-based vesicular solution (400 μg/mL) adsorbed on a mica (silicon) surface. The average heights were measured by cross section analysis for low-cholesterol (C) and high-cholesterol (F) vesicles, revealing the shape of a spherical cap.

Evaluation of redox sensitivity of the dendrimer-based vesicles

Size measurement

The bilayer of the dendrimer-based vesicles is composed of hydrophobic cholesterol, which is conjugated to the PEGylated dendrimer via a disulfide linkage sensitive to the reducing agent

glutathione (Scheme 2). The redox-responsiveness of these vesicles was investigated by monitoring the changes in the hydrodynamic sizes of the vesicles via dynamic light scattering measurements in presence or absence of glutathione at different time intervals and at different glutathione concentrations (10 μM and 10 mM, corresponding to reducing environments in the extracellular and intracellular compartments respectively).

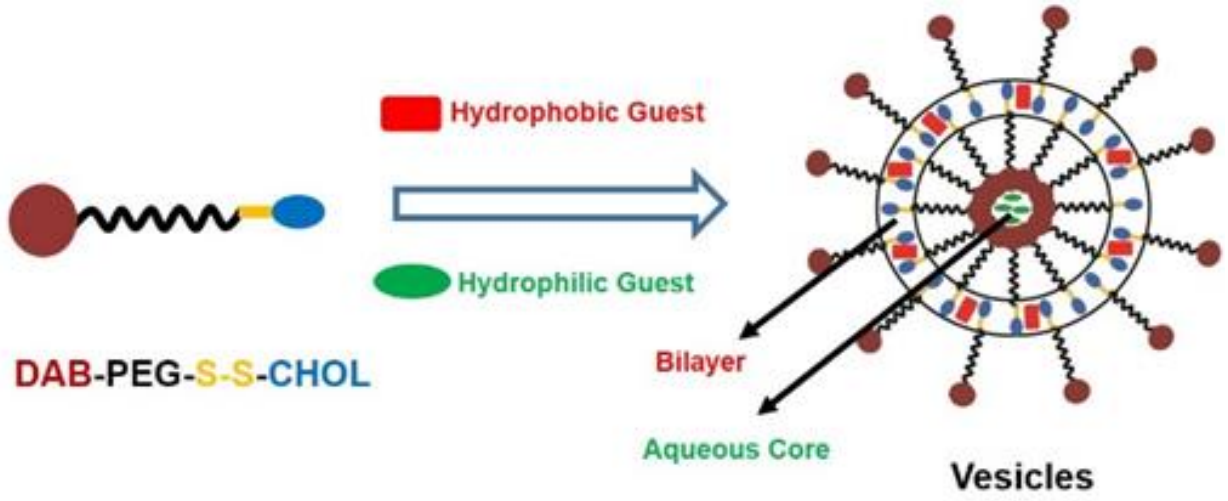

Scheme 2. Schematic representation of the formation of vesicles by both low-cholesterol and high-cholesterol DAB-PEG-S-S-CHOL dendrimers, showing encapsulation of hydrophilic and hydrophobic drugs respectively in the aqueous core and hydrophobic bilayer.

Low-cholesterol vesicles displayed similar sizes (less than 200 nm) in presence of 10 μM or without glutathione at all the tested durations. However, a higher concentration (10 mM) of glutathione induced a pronounced increase in size from 9 h (104.3 ± 15.2 nm) to 48 h (716.3 ± 16.1 nm), therefore demonstrating that the vesicles have disintegrated at that time (Figure 6A).

A similar trend was also observed for the high-cholesterol vesicles in presence of 10 mM glutathione from 9 h (155.1 ± 66.1 nm) to 48 h (771.1 ± 28.2 nm) although the vesicle size at 24

h (240.3 ± 78.3 nm) was lower than that observed with low-cholesterol vesicles (331.3 ± 37.2 nm) (Figure 6B). This increase in size can be attributed to the cleavage of the disulfide bonds and disintegration of the vesicles, forming larger, unstable and less compact aggregates. The high-cholesterol PEGylated dendrimer, having a larger amount of cholesterol and larger number of disulfide linkages than its low-cholesterol counterpart, may allow a more limited access for the hydrophilic glutathione to its lipidic bilayer (thus explaining the size differences at 24 h) and may require a larger amount of glutathione to break the excess disulphide bonds than low-cholesterol dendrimer. Both low-and high-cholesterol vesicles expressed strong redox sensitivity in presence of 10 mM glutathione, corresponding to reducing environment in the intracellular compartment. These effects were similar to those observed for redox-responsive PEGylated generation 4-PAMAM dendrimers (that show a significant decrease of particle size from 16.9 ± 0.8 nm to 12.5 ± 0.5 nm occurring in presence of 10 mM glutathione)[41] and disulphide cross-linked hyperbranched PAMAM dendrimer-based vesicles, whose size changed from 110 nm to 23 nm in presence of 10 mM dithiothreitol. [36]

The sizes of vesicles incubated in PBS with or without 10 μM glutathione were almost the same even 48 h after the start of the experiment, implying that the extracellular reducing environment has little effect on the integrity of the vesicles. However, the intracellular or cytosolic reducing environment (corresponding to 10 mM glutathione) has a massive impact on the disassembly of the vesicles, raising the possibility of future use of these dendrimer-based vesicles as redox-responsive drug delivery systems for cancer treatment, as cancer cells have even further elevated intracellular glutathione concentration.

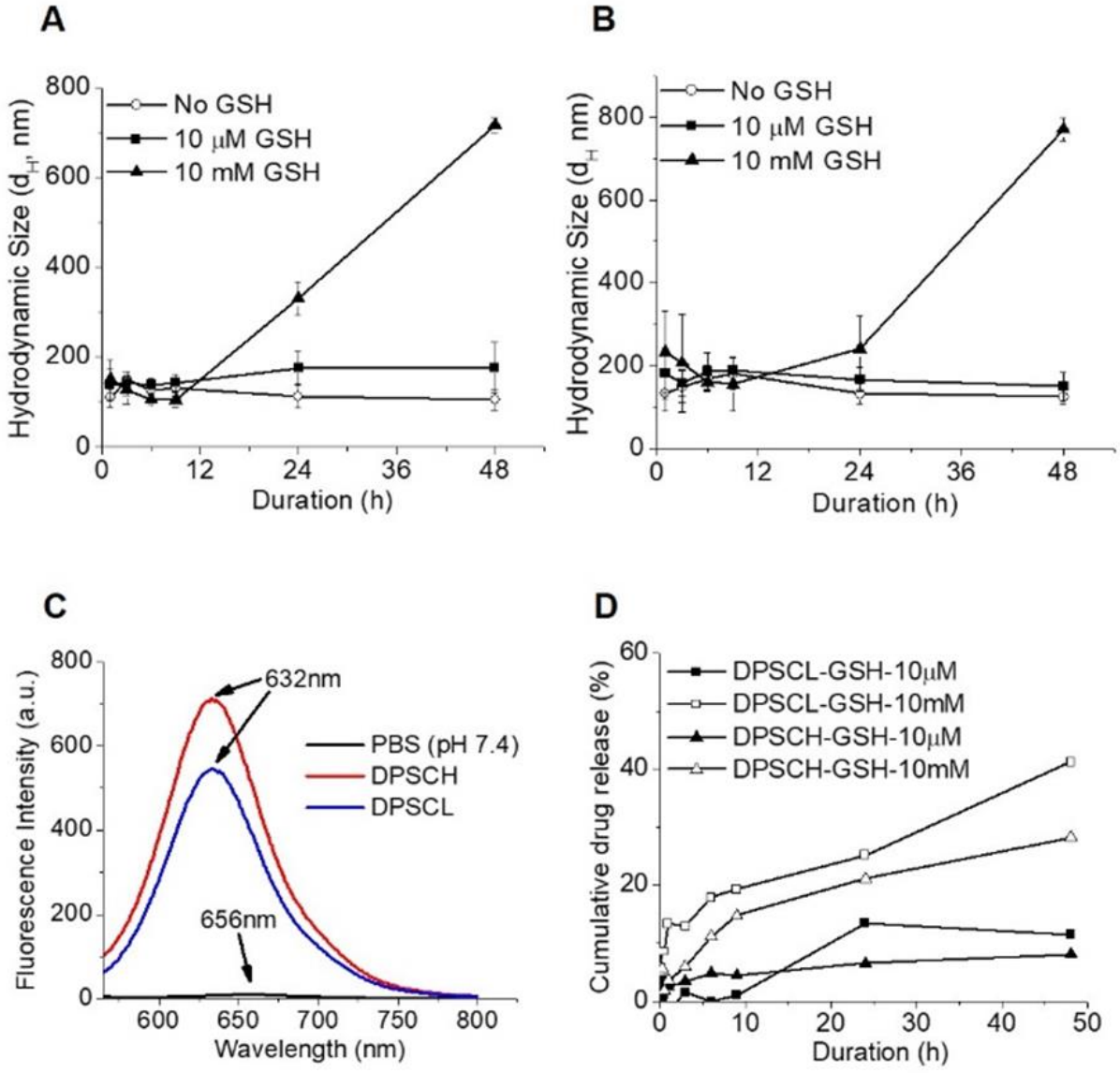

Figure 6. Evaluation of gluthatione sensitivity of the dendrimer-based vesicles:

- Hydrodynamic size distribution of low-cholesterol (A) and high-cholesterol (B) dendrimer-based vesicles (100 μg/mL in PBS, pH 7.4) at different time intervals, in presence or in absence of glutathione (GSH) (10 μM and 10 mM) at 37 ºC (n=3)

- Fluorescence emission spectra of Nile Red in PBS (pH 7.4) (C), alone or in presence of low-cholesterol (DPSCL) and high-cholesterol (DPSCH) dendrimer-based vesicles (100 µg/mL in PBS, pH 7.4)

- Release profile of Nile Red (D) from low-cholesterol (DPSCL) and high-cholesterol (DPSCH) dendrimer-based vesicles (100 µg/mL in PBS, pH 7.4), in absence or presence of GSH (10 µM and 10 mM) at different time intervals.

Redox-sensitive release of Nile Red from the vesicles

The successful entrapment of Nile Red in the bilayer of the vesicles (with drug loading efficiencies of respectively 0.14 % and 0.17 % for low- and high-cholesterol dendrimer-based vesicles) was shown by an increase in fluorescence intensity of Nile Red in presence of the vesicles (543, 703 and 10 fluorescence arbitrary units respectively with low-cholesterol vesicles, high-cholesterol vesicles and free Nile Red solution), with a concomitant blue shift of 24 nm for λ_{max} of the entrapped dye (λ_{max}: 632 nm) compared to the free solution (λ_{max}: 656 nm) (Figure 6C). The increased fluorescence intensity observed in the presence of high-cholesterol vesicles might be attributed to the higher cholesterol content of these vesicles, thus facilitating the entrapment of the lipophilic dye in the lipid bilayer of the vesicles.

In presence of glutathione, a tripeptide having a free thiol, the vesicle bilayers are expected to be disassembled due to thiol-disulphide reaction, with a concomitant release of the encapsulated Nile Red.[45] This naturally occurring biological thiol is present at different concentrations in extracellular (10 µM) and intracellular (10 mM) compartments. The fluorescence intensity of the entrapped Nile Red was monitored in function of time in presence or absence of glutathione (10 µM and 10 mM). The fluorescence intensity of Nile Red entrapped in low-cholesterol- and high-

cholesterol-vesicles sharply decreased in presence of 10mM glutathione (Figure S8). This effect was most pronounced at 48 h after the start of the incubation with the low-cholesterol vesicles (299 and 486 arbitrary units for Nile Red respectively entrapped in low-and high-cholesterol vesicles). The decrease of fluorescence intensity was also observed in the presence of 10 μM glutathione, but to a lesser extent (453 and 620 arbitrary units for Nile Red respectively entrapped in low-and high-cholesterol vesicles at 48 h).

The cumulative release profile of Nile Red from the vesicles in presence or absence of glutathione indicated that both vesicles are more fragile in intracellular redox conditions rather than in extracellular conditions, leading to a higher and faster release of Nile Red in more reductive conditions (up to 40% and ~ 25% Nile red release from respectively the low-cholesterol and high-cholesterol dendrimersomes in presence of 10 mM glutathione) (Figure 6D). Although both low- and high-cholesterol vesicles showed a sustained release of the dye, the high-cholesterol vesicles having more disulphide-conjugated lipophilic units were more resistant to higher glutathione concentration, resulting in a lower release of the guest compared to its low-cholesterol counterpart. The sustained release of the hydrophobic Nile Red dye may be due to the limited access of the hydrophilic glutathione to the highly hydrophobic and compact bilayer region of the vesicles and would be advantageous for the slow release of a drug in conjunction with an associated therapeutic entity with a faster release, such as therapeutic nucleic acid. These results were close to that observed with redox-sensitive PEGylated amphiphilic methacrylate-based polymeric nanoassemblies without any cholesterol (up to 40% Nile Red release when in presence of 10 mM glutathione). [45]

Characterization of dendriplex formation

Evaluation of DNA condensation

The cholesterol-bearing PEGylated dendrimers can efficiently bind to negatively charged DNA through electrostatic interactions between the protonated primary amines of the dendrimers and the negatively charged phosphodiester groups of the DNA to form dendrimer: DNA complexes (dendriplexes). The fluorescence of PicoGreen® significantly increases on intercalation with double stranded DNA. The electrostatic interactions between the negatively charged DNA and positively charged dendrimers on formation of the dendriplex condense the DNA and reduce the number of PicoGreen® binding sites, resulting in a decrease in the fluorescence intensity of the PicoGreen® solution.

Both low-cholesterol and high-cholesterol dendrimers were able to condense more than 85% of the DNA at all tested ratios for the low-cholesterol dendrimer, and at dendrimer: DNA weight ratios of 1:1 and higher for the high-cholesterol dendrimer, which displayed less primary amines at its periphery than its low-cholesterol counterpart (Figures 7A and B). DNA condensation occurred instantly and was found to be stable for at least 24 h. DNA condensing ability of these modified dendrimers was of the same range to that reported for generations 1, 2 and 3-PAMAM dendrimers conjugated to 40% cholesterol, [30-31] PEGylated poly(amidoamine) dendron-bearing lipids-based lipoplexes, [16] octadecyl alkyl chain-bearing generations 2- and 3- PAMAM dendrons forming lipoplexes following probe sonication [46] (up to 100% for all of these formulations).

A gel retardation assay confirmed the complete and partial DNA condensation by cholesterol-bearing dendrimers (Figures S9 and S10). At dendrimer: DNA weight ratios higher than 1:1,

DNA was fully condensed by cholesterol-bearing DAB, thus preventing ethidium bromide to intercalate with DNA. No free DNA was therefore visible at these ratios.

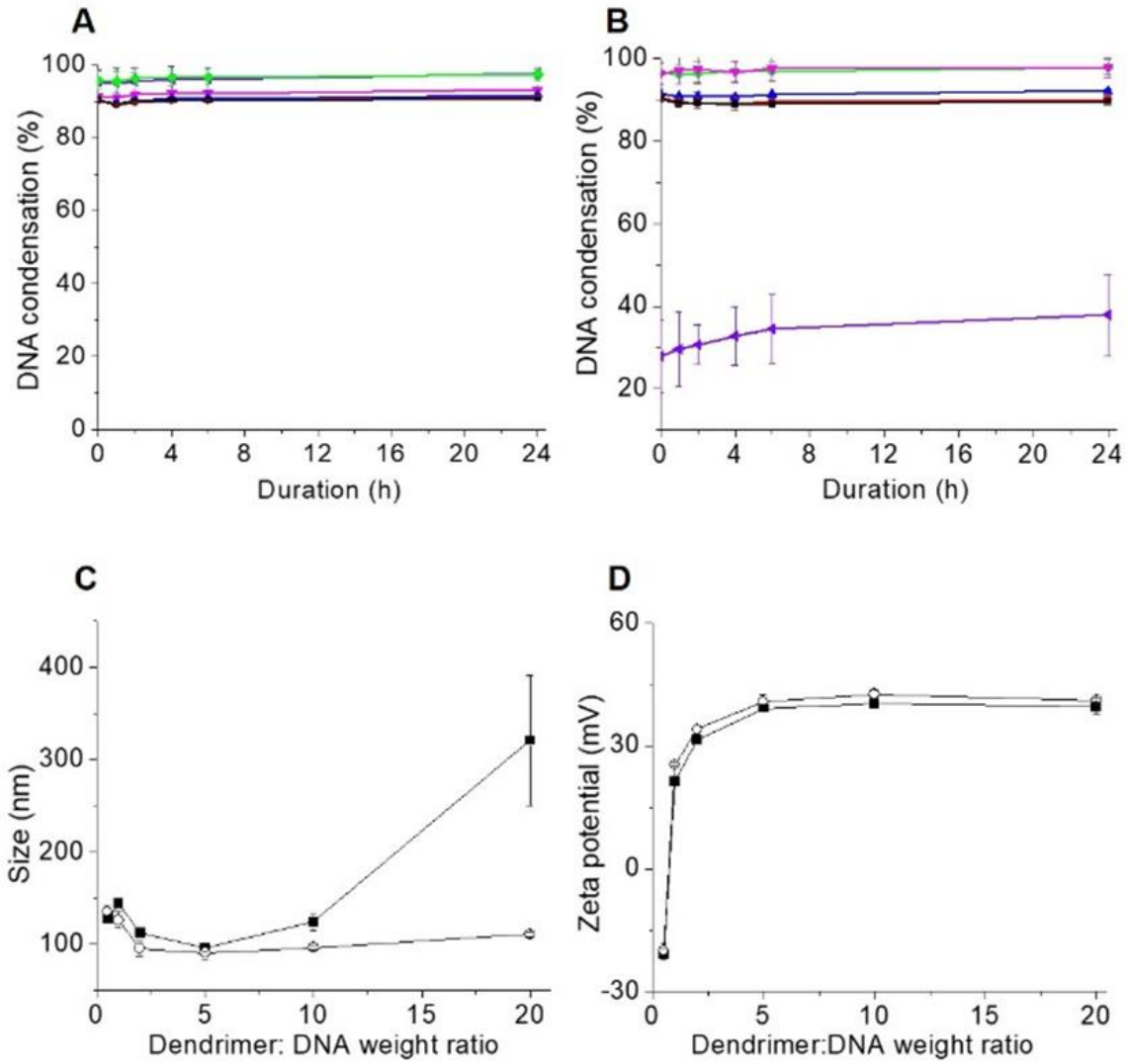

Figure 7. Evaluation of the DNA complexation of the low-cholesterol and high-cholesterol dendrimers:

- DNA condensation of low-cholesterol (A) and high-cholesterol (B) dendriplexes using PicoGreen® reagent at various durations and dendrimer: DNA weight ratios: 20:1 (■, black), 10:1 (●, red), 5:1 (▲, blue), 2:1 (▼, magenta), 1:1 (♦, green) and 0.5:1 (◄, violet). Results are expressed as mean ± SEM (n=4)

- Size (C) and zeta potential (D) of low-cholesterol (○) and high-cholesterol (■) dendriplexes at various dendrimer: DNA weight ratios, in 5% glucose at 37 ºC (n=3)

Size and zeta potential measurement

Low-cholesterol dendriplex displayed an average size lower than 150 nm at all dendrimer: DNA weight ratios used, with a low polydispersity index (0.15 to 0.3). By contrast, the size of high-cholesterol dendriplex initially decreased with increasing dendrimer: DNA weight ratios ranging from 0.5:1 to 5:1 (from 127.6 ± 3.7 nm to 95.8 ± 4.2 nm) due to the increase in hydrophobicity, as previously described in the case of cholesterol modified spermine-functionalised dendrons. [47] It then increased to reach a maximum of 320.8 ± 70.2 nm at a ratio of 20:1 which might be due to losing its hydrophobic balance (Figure 7C).

Overall, dendriplexes showed a smaller hydrodynamic diameter due to the presence of the highly hydrophobic cholesterol in the backbone, leading to the formation of more compact dendriplexes in comparison to not only C18 alkyl chain-modified generation 3- PAMAM dendrimers, but also cholesterol-modified generations 1, 2 and 3- PAMAM-based dendriplexes.[16,30-31] Both low-cholesterol and high-cholesterol dendriplexes presented an overall average size lower than the unmodified DAB dendriplex, which had an average size of 196 nm (polydispersity index: 0.683). [8] This smaller size will further facilitate their extravasation to cancer cells.

Zeta potential experiments demonstrated that the dendriplexes were bearing slightly increasing positive surface charge comprised between 21.4 ± 0.9 and 41.1 ± 0.6 mV for most ratios, but a negative charge of around –20 mV at a dendrimer: DNA weight ratio of 0.5:1. There was no significant differences of results between low- and high-cholesterol dendriplexes (Figure 7D). These dendriplexes showed a much higher positive zeta potential in comparison with PEGylated poly(amidoamine) dendron-bearing lipids-based lipoplexes (~4-10 mV) [25] and with generations

1, 2 and 3-PAMAM dendrimers conjugated to 40% cholesterol (~18-23 mV).[30-31] This increased zeta potential would therefore further facilitate the uptake of these dendriplexes by cancer cells.

Observation of the morphology of the dendriplexes

Transmission electron microscopic images showed the presence of dendrimer-based vesicles even after complexation with DNA, at dendrimer: DNA weight ratios 5:1 and 10:1 (Figure 8). Both the dendrimers have retained their ability to form vesicles with sizes lower than 100 nm in presence of DNA, unlike other C17 alkyl chain-modified polyamine-based dendrimersomes that transformed from vesicular forms to micellar structures in presence of siRNA.[34] Low-cholesterol vesicles appeared to form smaller vesicles at a ratio 5:1 than at a ratio 10:1, unlike the high-cholesterol vesicles that seemed to be of similar size at both ratios.

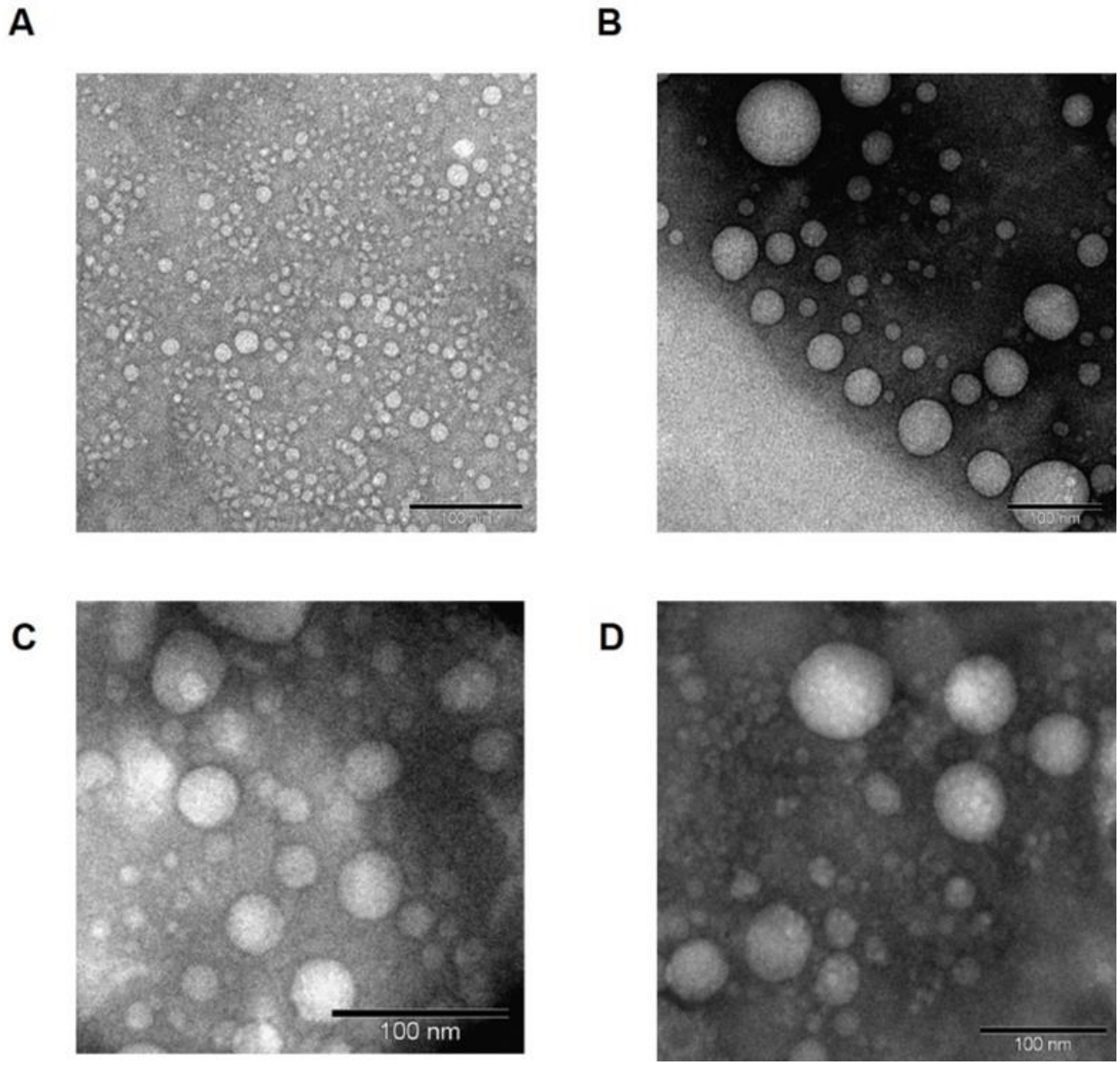

Figure 8. Unstained TEM images of low-cholesterol (A and B) and high-cholesterol (C and D) dendriplexes at dendrimer: DNA weight ratios of 5:1 (A and C) and 10:1 (B and D)

In vitro analysis

Evaluation of cell viability

The viability of PC-3 cells following treatment with low-cholesterol vesicles was maintained up to a dendrimer concentration of 40 µg/mL for 24 h incubation (58.7 ± 12.6 % viability) and 25 µg/mL for 48 h and 72 h incubation (64.5 ± 11.1 and 56.7 ±17.6 % viability respectively) (Figure 9A).

Replacing low-cholesterol dendrimersomes with high-cholesterol dendrimersomes led to a decrease in cell viability, which remains constant up to a dendrimer concentration of 35 µg/mL for 24 h and 48 h incubation (71.9 ± 10.4 and 66.4 ± 11.4 % viability respectively) and 40 µg/mL for 72 h incubation (66.4 ± 8.9 % viability) (Figure 9B). Similar cell viability was observed following treatment of HeLa-Luc cells and Huh-7-Luc cancer cell lines with cationic PAMAM dendron-bearing lipids (more than 70% viability up to 32 µg/mL after 48 h). [48] Low- and high-cholesterol dendrimersomes led to an improved cell viability compared with cholesterol-modified generations 3- and 5- PAMAM dendrimers [49], which might be due to the presence of PEG and comparatively lower amount of cholesterol in the backbone.

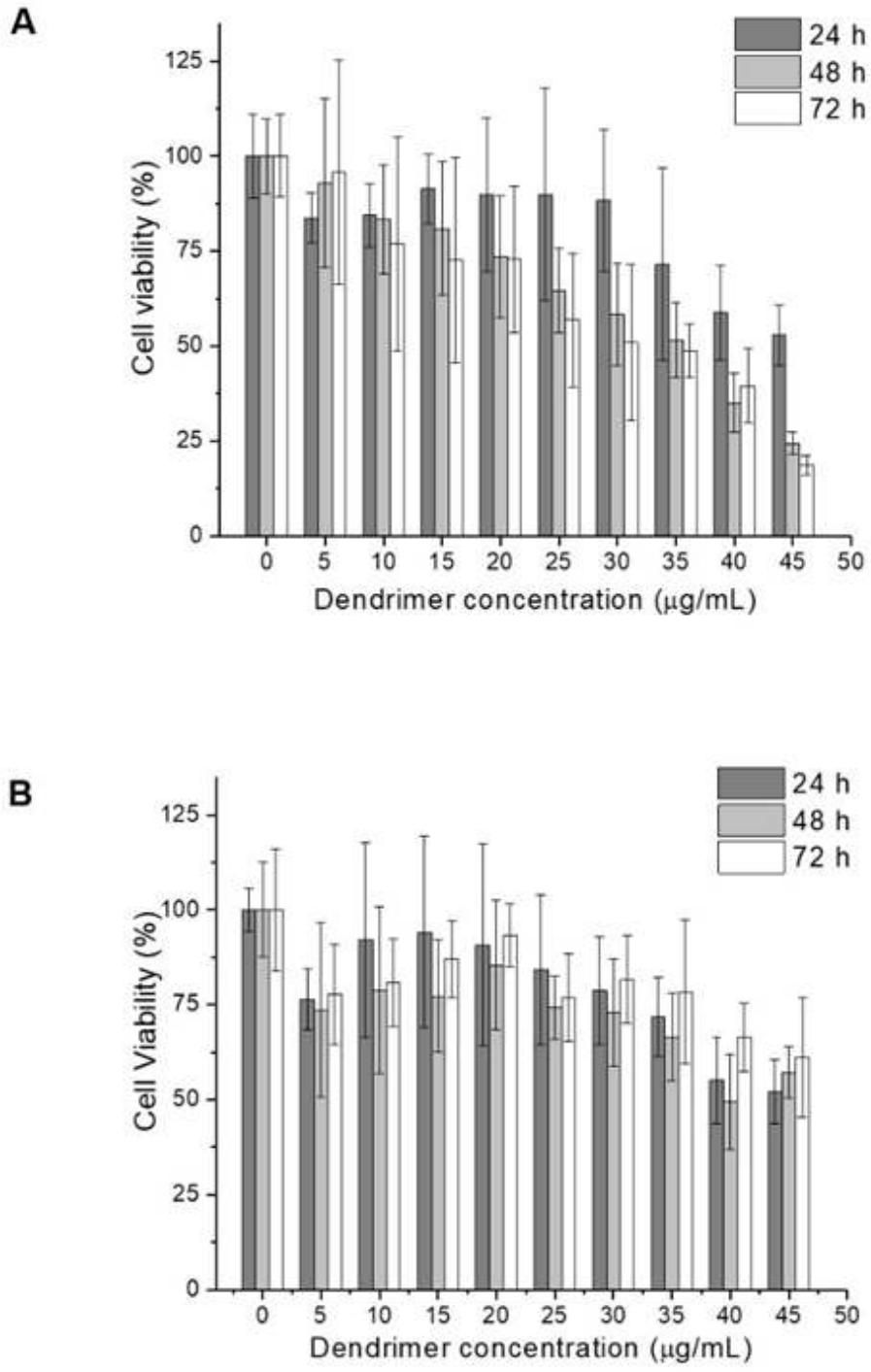

Figure 9. Cell viability of the low-cholesterol (A) and high-cholesterol (B) dendrimers on PC3 prostate cancer cells at various concentrations and treatment durations (n=6) (* : P <0.05 compared with dendrimer concentration at t= 0 h)

Evaluation of gene expression of the dendrimers complexed with DNA

Both low-and high-cholesterol dendrimers complexed to DNA led to gene transfection at all the durations tested on PC3 cell line with different amounts (Figure 10). The highest transfection level following treatment with low-cholesterol dendrimer complex was obtained at dendrimer: DNA weight ratio of 5:1 after 72 h treatment. At this ratio, gene expression was 4.92-fold higher than following treatment with DNA (1.30 ± 0.07 U/mL), but 1.33-fold lower than with DAB dendriplex (8.55 ± 0.64 U/mL).

When replacing low-cholesterol dendrimer by high-cholesterol dendrimer, the highest gene expression resulted from treatment with the dendrimer complex at a ratio of 10:1, after 72 h treatment. It was 4.98-fold higher than following treatment with DNA (1.2 ± 0.15 U/mL), 1.26-fold lower than with DAB dendriplex (7.59 ± 1.38 U/mL), and similar to the highest gene expression obtained with its low-cholesterol counterpart. Treatment with naked DNA only resulted in weak levels of gene expression, as expected. Both cholesterol-modified DAB-dendriplexes showed slightly less transfection efficacy compared with unmodified DAB dendriplex after 3 days of treatment. This might be due to a decrease in proton sponge effect, occurring as a consequence of the substitution on the dendrimers. As cholesterol has previously been shown to disrupt endosomal membrane [47], another possibility would be that the dendrimers should be conjugated to an even higher amount of cholesterol to increase their gene expression ability. This hypothesis is further reinforced by the fact that all the generation 1-, generation 2- and generation 3-PAMAM dendrimers conjugated to cholesterol at 40% mole ratio of cholesterol/primary amine displayed a significantly higher gene expression than their unmodified dendriplexes.[30-31]

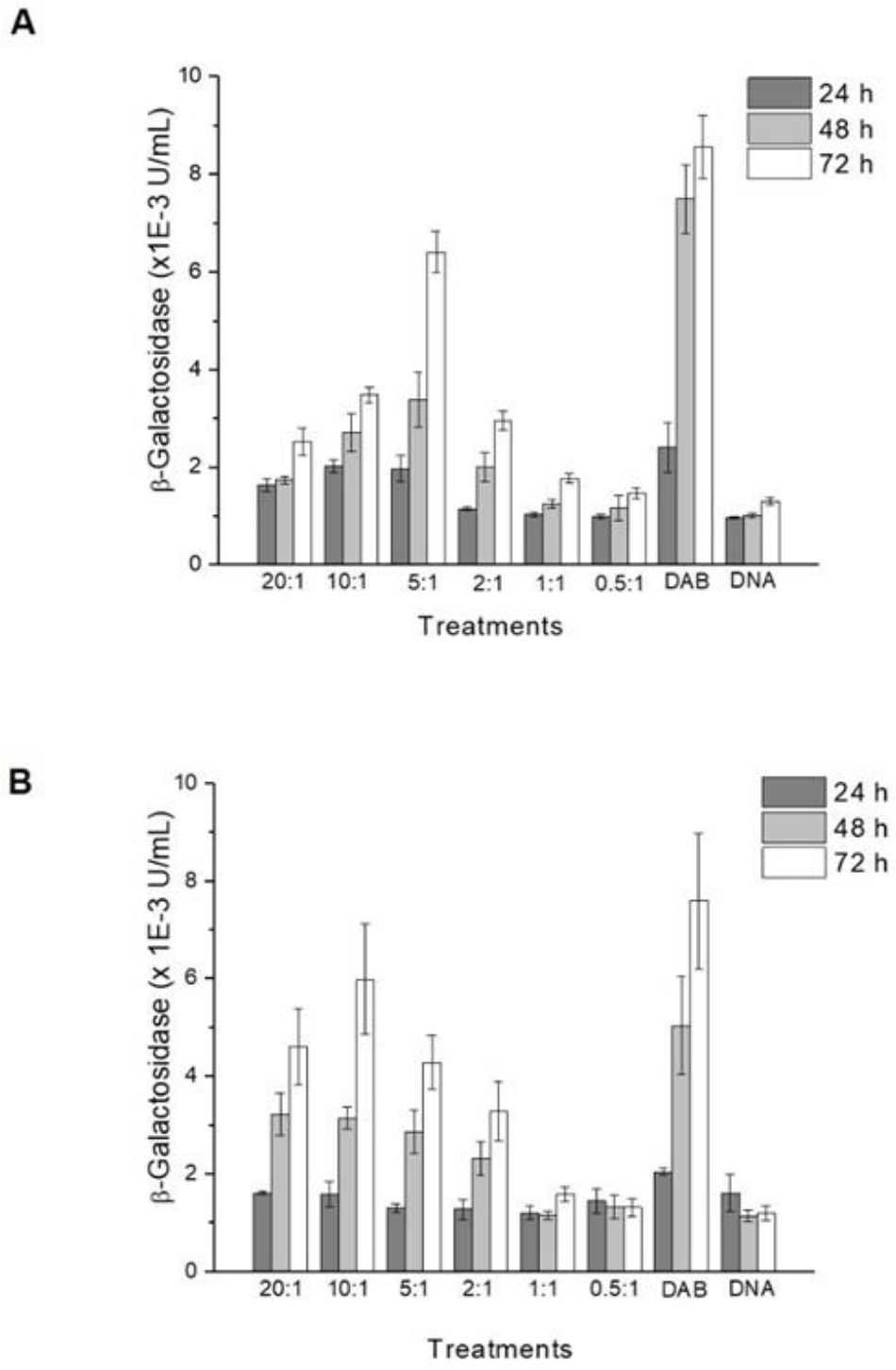

Figure 10. Transfection efficacy of low-cholesterol (A) and high-cholesterol (B) dendriplexes at various dendrimer: DNA weight ratios in PC3 prostate cancer cells. (Optimal DAB: DNA ratio:

5:1) (n=5) (A: P <0.05 for all treatments compared with DAB, B: only 10:1 treatment was not significantly different from DAB treatment)

Cellular uptake of dendriplexes

Qualitative analysis

The cellular uptake of the complex formed between fluorescein-labeled DNA and dendrimer-based vesicles, was qualitatively confirmed in PC-3 cells using confocal microscopy (Figure 11). Fluorescein-labeled DNA was disseminated in the cytoplasm of the cells after treatment with both low-and high-cholesterol vesicles, at both 5:1 and 10:1 ratios. The DNA uptake appeared to be the highest following treatment with high-cholesterol vesicles at a dendrimer: DNA weight ratio of 10:1. It also appeared to be more pronounced in the cells treated with the vesicle complexes than with DAB dendriplex. No co-localization of DNA in the nuclei was visible after 2 h incubation.

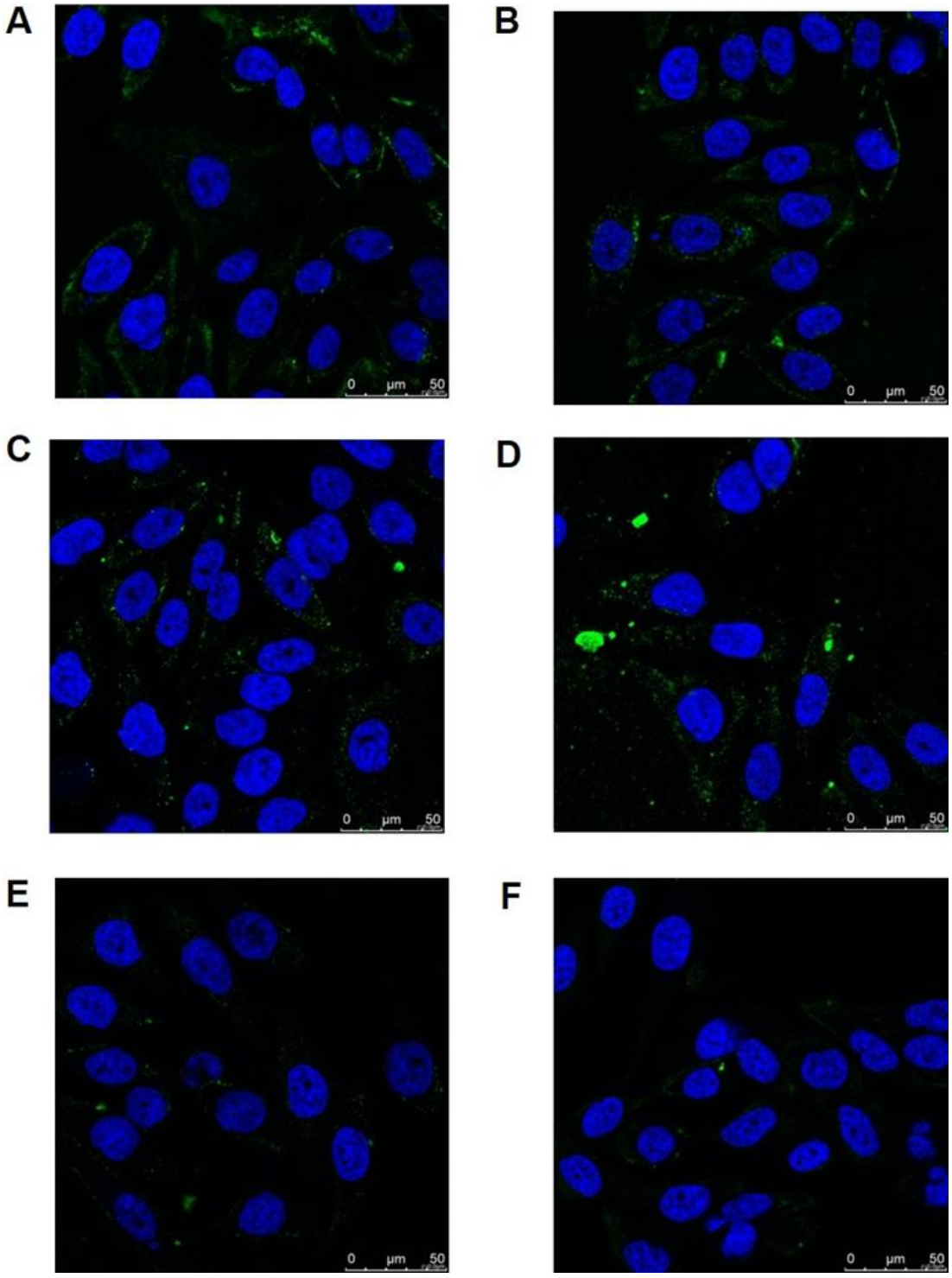

Figure 11. Confocal microscopy images of the cellular uptake of fluorescein-labelled DNA (2.5 µg/dish), complexed with low-cholesterol dendrimer (A: dendrimer: DNA ratio 5:1, B:

dendrimer: DNA ratio 10:1), high-cholesterol dendrimer (C: dendrimer: DNA ratio 5:1, D: dendrimer: DNA ratio 10:1), DAB dendrimer (E) or free in solution (F), after 2h incubation with PC3-Luc cells. Blue: nuclei stained with DAPI (excitation: 405 nm laser line, bandwidth: 415–491 nm), green: fluorescein-labelled DNA (excitation: 453 nm laser line, bandwidth: 550–620 nm) (Magnification: ×40).

Quantitative analysis

Qualitative results were quantitatively confirmed by flow cytometry. Treatment of PC3 cells with the low-cholesterol complex resulted in the highest cellular fluorescence at a dendrimer: DNA ratio of 5:1 (3970 ± 184 arbitrary units (a.u.)), which was respectively 12.5-fold and 15.4-fold higher than that observed after treatment with DAB dendriplex (315 ± 10.50) and DNA solution (257 ± 6 a.u.) (Figures 12 and S11). It was also 1.3-fold higher than that when using a dendrimer: DNA weight ratio of 10:1 instead of 5:1 (3022 ± 55 a.u.).

Increased cellular fluorescence was also observed following treatment with high-cholesterol complex at a 10:1 ratio (2775 ± 81 a.u.). It was respectively 8.8-fold and 10.78-fold higher than that observed following treatment with DAB dendriplex and DNA solution, but also 1.9-fold higher than when using a ratio of 5:1 (1414 ± 63 a.u.). In addition, treatment of the cells with naked DNA resulted in a weak DNA uptake, demonstrating the failure of DNA to be taken up by prostate cancer cells without the assistance of a carrier.

This enhanced delivery of DNA to the cancer cells most likely resulted from the highly positive charges of the dendriplexes, as positive charges increase their electrostatic interactions with the negatively charged cellular membranes and facilitate cellular uptake. [37] However, this

did not result in an increased expression of the reporter gene compared with the unmodified DAB dendriplex.

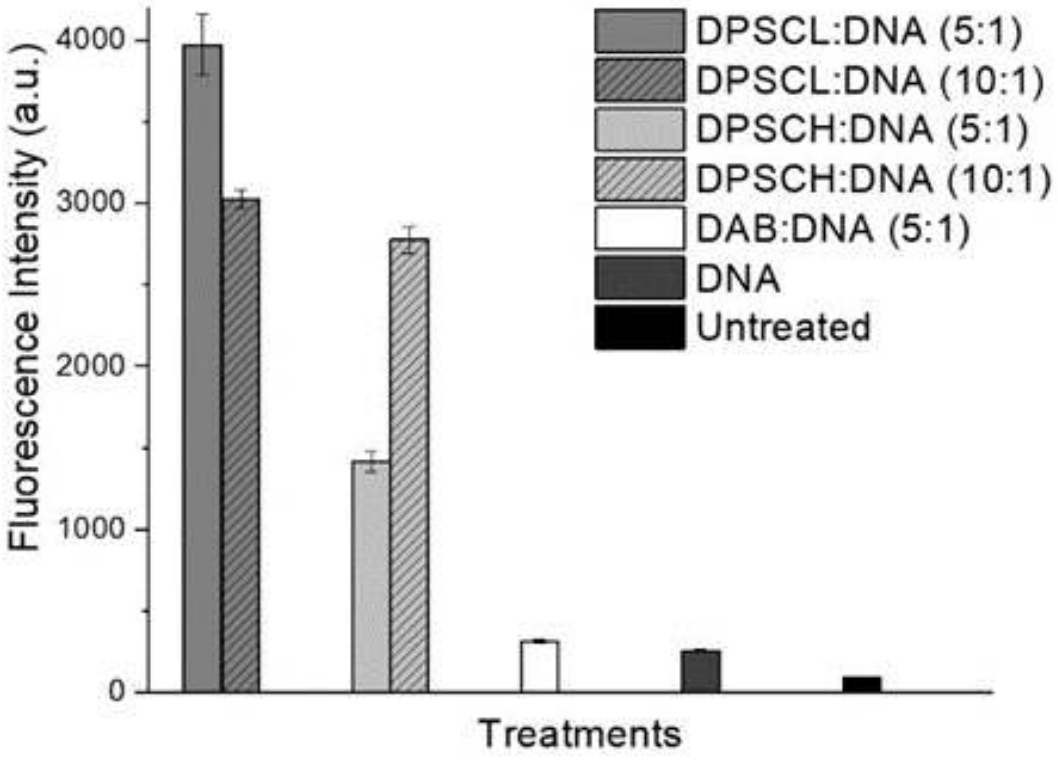

Figure 12. Quantification of the cellular uptake of fluorescein-labeled DNA (2.5 μg/well), complexed with low- or high-cholesterol dendrimers (DPSCL and DPSCH respectively), DAB dendrimer, or free in solution, after 2 h incubation with PC3-Luc cells, using flow cytometry (n=3) (*: $P < 0.05$ compared with DAB-DNA)

To the best of our knowledge, this is the first report on cholesterol-bearing PEGylated polypropylenimine dendrimers forming spontaneous, redox-sensitive, cationic stable vesicles

able to carry hydrophilic or hydrophobic compounds as well as DNA, leading to gene expression in prostate cancer cells. Other cholesterol-modified dendrimers have previously been reported (spermine-functionalized dendrons conjugated with cholesterol [47], cholesterol-conjugated PAMAM dendrimers) [30-31, 49], but for use as a non-viral gene delivery system only, and without redox sensitivity. Amphiphilic dendrimers based on polypropylenimine dendrimers have also been shown to self-assembly, but without redox-sensitivity or entrapment of any drugs or genes. [50] Redox-responsive PAMAM has previously been reported as delivery systems, but to deliver either DNA or hydrophobic drug, and this without the formation of vesicles. [51-52] These novel cholesterol-bearing PEGylated poly(propylene imine) dendrimer-based vesicles therefore hold promising prospects as redox-sensitive drug and gene delivery systems for cancer therapy.

CONCLUSION

In this proof of concept study, two disulphide-linked cholesterol-bearing PEGylated dendrimers have been successfully synthesized through *in situ* two-step reaction. Both the low and high cholesterol-bearing dendrimers were able to spontaneously self-assemble into stable vesicles in PBS (pH 7.4), with lower critical aggregation concentration values for high cholesterol-bearing vesicles. These cationic, nano-sized vesicles, or dendrimersomes, were able to entrap both hydrophilic and hydrophobic guests, and also showed a redox-responsive sustained release of the entrapped guests at higher glutathione concentration corresponding to reducing environment in the intracellular compartment. In addition, both dendrimeric vesicles were able to condense more than 85 % of the DNA at all tested ratios for the low-cholesterol vesicles, and at dendrimer: DNA weight ratios of 1:1 and higher for the high-cholesterol vesicles. These vesicles resulted in an enhanced cellular uptake of DNA, by up to 15-fold compared with naked DNA with the low-cholesterol vesicles. Consequently, they increased gene transfection on PC3 prostate cancer cell line, with the highest transfection being obtained with low-cholesterol vesicle complex at a dendrimer: DNA weight ratio of 5:1 and high-cholesterol vesicle complex at a dendrimer: DNA weight ratio of 10:1. These transfection levels were about 5-fold higher than that observed when treated with naked DNA. These novel cholesterol-bearing PEGylated dendrimer-based vesicles are therefore very promising as redox-sensitive drug and gene delivery systems for future applications in cancer therapy.

ASSOCIATED CONTENT

Figures S1- S11, Table S1 (PDF)

AUTHOR INFORMATION

Corresponding Author

* Corresponding author: Christine Dufès

Strathclyde Institute of Pharmacy and Biomedical Sciences, University of Strathclyde, 161 Cathedral Street, Glasgow G4 0RE, United Kingdom

Phone: 44 -141 548 3796

Fax: 44 -141 552 2562

E-mail: C.Dufes@strath.ac.uk

Notes

The authors declare no competing financial interest.

ACKNOWLEDGMENT

This work was financially supported by a grant from Worldwide Cancer Research [grant number 16-1303] to C.D. and H.Y.L. P.L. and S.S. are respectively funded by research grants from Worldwide Cancer Research [grant number 16-1303] and The Dunhill Medical Trust [grant number R463/0216]. N.A. is in receipt of a PhD studentship from the Saudi Cultural Bureau and Princess Nourah bint Abdulrahman University (Kingdom of Saudi Arabia) [grant number 15678].

The authors would like to acknowledge CMAC National Facility, housed within the University of Strathclyde's Technology and Innovation Centre, and funded with a UK Research Partnership Institute Fund (UKRPIF) for the access to the AFM instrument and thermal analysis.

REFERENCES

1. Luo, D.; Saltzman, W. M. Synthetic DNA delivery systems. *Nat. Biotechnol.* **2000***,* 18, 33-37.
2. Liu, M.; Fréchet, J. M. J. Designing dendrimers for drug delivery. *Pharm. Sci. Technol. Today* **1999,** 2, 393-401.
3. Maeda, H.; Matsumura, Y. A new concept in macromolecular therapeutics in cancer chemotherapy: mechanism of tumoritropic accumulation of proteins and the antitumor agent SMANCS. *Cancer Res*. **1986**, 46, 6387–9392.
4. de Lima, M. C. P.; Simoes, S.; Pires, P.; Faneca, H.; Duzgunes, N. Cationic lipid-DNA complexes in gene delivery: from biophysics to biological applications. *Adv. Drug Delivery Rev.* **2001**, 47, 277−294.
5. Luo, K.; Li, C.; Li, L.; She, W.; Wang, G.; Gu, Z. Arginine functionalized peptide dendrimers as potential gene delivery vehicles. *Biomaterials.* **2012,** 33(19), 4917-27.
6. Luo, K.; He, B.; Wu, Y.; Shen, Y.; Gu, Z. Functional and biodegradable dendritic macromolecules with controlled architectures as nontoxic and efficient nanoscale gene vectors. *Biotechnol Adv.* **2014,** 32, 818-30.
7. Zinselmeyer, B. H.; Mackay, S. P.; Schätzlein, A. G.; Uchegbu, I. F. The lower-generation polypropylenimine dendrimers are effective gene-transfer agents. *Pharm. Res.* **2002**, 19, 960-967.
8. Koppu, S.; Oh, Y. J.; Edrada-Ebel, R.; Blatchford, D. R.; Tetley, L.; Tate, R. J.; Dufès, C. Tumor regression after systemic administration of a novel tumor-targeted gene delivery system carrying a therapeutic plasmid DNA. *J. Control. Release* **2010**, 143, 215-221.

9. Lemarié, F.; Croft, D. R.; Tate, R. J.; Ryan, K. M.; Dufès C. Tumor regression following intravenous administration of a tumor-targeted p73 gene delivery system. *Biomaterials* **33**, 2012, 2701-2709.

10. Al Robaian, M.; Chiam, K. Y.; Blatchford, D. R.; Dufès, C. Therapeutic efficacy of intravenously administered transferrin-conjugated dendriplexes encoding TNF-α, TRAIL and interleukin-12 on prostate carcinomas. *Nanomedicine (Lond.)* 9, 2014, 421-434.

11. Lim, L. Y.; Koh, P. Y.; Somani, S.; Al Robaian, M.; Karim, R.; Yean, Y. L.; Mitchell, J.; Tate, R. J.; Edrada-Ebel, R.; Blatchford, D. R.; Mullin, M.; Dufès C. Tumor regression following intravenous administration of lactoferrin- and lactoferricin-bearing dendriplexes. *Nanomedicine* 11, 2015, 1445-1454.

12. Altwaijry, N.; Somani, S.; Parkinson, J. A.; Tate, R. J.; Keating, P.; Warzecha, M.; Mackenzie, G. R.; Leung, H. Y.; Dufès C. Regression of prostate tumors after intravenous administration of lactoferrin-bearing polypropylenimine dendriplexes encoding TNF-α, TRAIL and interleukin-12. *Drug Deliv.* 25, 2018, 679-689.

13. Criscione, J. M.; Le, B. L.; Stern, E.; Brennan, M.; Rahner, C.; Papademetris, X.; Fahmy, T. M. Self-assembly of pH-responsive fluorinated dendrimer-based particulates for drug delivery and noninvasive imaging. *Biomaterials* **2009**, 30, 3946-3955.

14. Filippi, M., Patrucco, D., Martinelli, J., Botta, M., Castro-Hartmann, P., Tei, L. and Terreno, E., Novel stable dendrimersome formulation for safe bioimaging applications. *Nanoscale* **2015**, 7, 12943-12954.

15. Wang, B. B.; Zhang, X.; Jia, X.R.; Li, Z.C.; Ji, Y.; Yang, L.; Wei, Y. Fluorescence and aggregation behavior of poly (amidoamine) dendrimers peripherally modified with

aromatic chromophores: the effect of dendritic architectures. *J. Am. Chem. Soc* **2004**, 126, 15180-15194.

16. Takahashi, T.; Kojima, C.; Harada, A.; Kono, K. Alkyl chain moieties of polyamidoamine dendron-bearing lipids influence their function as a nonviral gene vector. *Bioconjug. Chem*, **2007**, 18, 1349-1354.
17. Zhang, P.; Xu, X.; Zhang, M.; Wang, J.; Bai, G.; Yan, H. Self-aggregation of amphiphilic dendrimer in aqueous solution: The effect of headgroup and hydrocarbon chain length. *Langmuir* **2015**, 31, 7919-7925.
18. Laskar, P.; Samanta, S.; Ghosh, S. K.; Dey, J. *In vitro* evaluation of pH-sensitive cholesterol-containing stable polymeric micelles for delivery of camptothecin. *J. Colloid Interface Sci.* **2014**, 430, 305-314.
19. Bajani, D.; Laskar, P.; Dey, J. Spontaneously formed robust steroidal vesicles: physicochemical characterization and interaction with HSA. *J. Phy.s Chem. B.* **2014**, 118, 4561-4570.
20. Ercole, F.; Whittaker, M. R.; Quinn, J. F.; Davis, T. P. Cholesterol modified self-assemblies and their application to nanomedicine. *Biomacromolecules* **2015**, 16, 1886-1914.
21. Yang, J.; Zhang, Q.; Chang, H.; Cheng, Y. Surface-engineered dendrimers in gene delivery. *Chem Rev.* **2015**, 115, 5274-5300.
22. Davis, F. F. The origin of pegnology. *Adv. Drug Deliv. Rev.* **2002**, 54, 457-458.
23. Photos, P. J.; Bacakova, L.; Discher, B.; Bates, F. S.; Discher, D. E. Polymer vesicles *in vivo*: correlations with PEG molecular weight. *J. Control. Release* **2003**, 90, 323-334.

24. Kim, Y.; Klutz, A. M.; Jacobson, K. A. Systematic investigation of polyamidoamine dendrimers surface-modified with poly (ethylene glycol) for drug delivery applications: synthesis, characterization, and evaluation of cytotoxicity. *Bioconjug. Chem.* **2008**, 19, 1660-1672.

25. Takahashi, T.; Hirose, J.; Kojima, C.; Harada, A.; Kono, K. Synthesis of poly (amidoamine) dendron-bearing lipids with poly (ethylene glycol) grafts and their use for stabilization of nonviral gene vectors. *Bioconjug. Chem.* **2007**, 18, 1163-1169.

26. Somani, S.; Laskar, P.; Altwaijry, N.; Kewcharoenvong, P.; Irving, C.; Robb, G.; Pickard, B. S.; Dufès, C. PEGylation of polypropylenimine dendrimers: effects on cytotoxicity, DNA condensation, gene delivery and expression in cancer cells. *Sci. Rep*. **2018**, 8, 9410.

27. Huo, M.; Yuan, J.; Tao, L.; Wei, Y. Redox-responsive polymers for drug delivery: from molecular design to applications. *Polym. Chem.* **2014**, 5, 1519-1528.

28. Hrkach, J. S.; Peracchia, M. T.; Bomb, A.; Langer, R. Nanotechnology for biomaterials engineering: structural characterization of amphiphilic polymeric nanoparticles by 1H NMR spectroscopy. *Biomaterials* **1997**, 18, 27-30.

29. Laskar, P.; Saha, B.; Ghosh, S. K.; Dey, J. PEG based random copolymer micelles as drug carriers: the effect of hydrophobe content on drug solubilization and cytotoxicity. *RSC Adv.* **2015**, 5, 16265-16276.

30. Golkar, N.; Samani, S. M.; Tamaddon, A. M. Cholesterol-conjugated supramolecular assemblies of low generations polyamidoamine dendrimers for enhanced EGFP plasmid DNA transfection. *J. Nanopart. Res.* **2016**, 18, 107.

31. Golkar, N.; Samani, S. M.; Tamaddon, A. M. Modulated cellular delivery of anti-VEGF siRNA (bevasiranib) by incorporating supramolecular assemblies of hydrophobically modified polyamidoamine dendrimer in stealth liposomes. *Int. J. Pharm.* **2016**, 510, 30-41.

32. Percec V.; Wilson D. A.; Leowanawat P.; Wilson C. J.; Hughes A. D.; Kaucher M. S.; Hammer D. A.; Levine D. H.; Kim A. J.; Bates F. S.; Davis K. P.; Lodge T. P.; Klein M. L.; DeVane R. H.; Aqad E.; Rosen B. M.; Argintaru A. O.; Sienkowska M. J.; Rissanen K.; Nummelin S.; Ropponen J. Self-assembly of Janus dendrimers into uniform dendrimersomes and other complex architectures. *Science* **2010**, 328, 1009-14.

33. Kono, K.; Murakami, E.; Hiranaka, Y.; Yuba, E.; Kojima, C.; Harada, A.; Sakurai, K. Thermosensitive Molecular Assemblies from Poly (amidoamine) Dendron-Based Lipids. *Angew. Chem. Int. Ed.* **2011**, 50, 6332-6336.

34. Liu, X.; Zhou, J.; Yu, T.; Chen, C.; Cheng, Q.; Sengupta, K.; Huang, Y.; Li, H.; Liu, C.; Wang, Y.; Posocco, P. Adaptive Amphiphilic Dendrimer-Based Nanoassemblies as Robust and Versatile siRNA Delivery Systems. *Angew. Chem. Int. Ed.* **2014**, 53, 11822-11827.

35. Yuan, F.; Dellian, M.; Fukumura, D.; Leunig, M.; Berk, D. A.; Torchilin, V. P.; Jain, R. K. Vascular permeability in a human tumor xenograft: molecular size dependence and cutoff size. *Cancer Res.* **1995**, 55, 3752-3756.

36. Nie, J.; Wang, Y.; Wang, W. *In vitro* and *in vivo* evaluation of stimuli-responsive vesicle from PEGylated hyperbranched PAMAM-doxorubicin conjugate for gastric cancer therapy. *Int. J. Pharm.* **2016**, 509, 168-177.

37. Mahato R. I.; Smith L. C.; Rolland A. Pharmaceutical perspectives of nonviral gene therapy. *Adv. Genet*. **1999**, 41, 95-156.

38. Laskar, P.; Dey, J.; Kumar Ghosh, S. Evaluation of zwitterionic polymersomes spontaneously formed by pH-sensitive and biocompatible PEG based random copolymers as drug delivery systems. *Colloids Surf. B Biointerfaces* **2016**, 139, 107-116.

39. Aathimanikandan, S. V.; Savariar, E. N.; Thayumanavan, S. Temperature-sensitive dendritic micelles. *J. Am. Chem. Soc.* **2005**, 127, 14922-14929.

40. Taylor, K. M.; Morris, R. M. Thermal analysis of phase transition behaviour in liposomes. *Thermochim. Acta* **1995**, 248, 289-301.

41. Chemin, M.; Brun, P. M.; Lecommandoux, S.; Sandre, O.; Le Meins, J. F. Hybrid polymer/lipid vesicles: fine control of the lipid and polymer distribution in the binary membrane. *Soft Matter* **2012**, 8, 2867-2874.

42. Jaskiewicz, K.; Makowski, M.; Kappl, M.; Landfester, K.; Kroeger, A. Mechanical properties of poly (dimethylsiloxane)-block-poly (2-methyloxazoline) polymersomes probed by atomic force microscopy. *Langmuir* **2012**, 28, 12629-12636.

43. Teschke, O.; De Souza, E. F. Liposome structure imaging by atomic force microscopy: verification of improved liposome stability during adsorption of multiple aggregated vesicles. *Langmuir* **2002**, 18, 6513-6520.

44. Hu, W.; Cheng, L.; Cheng, L.; Zheng, M.; Lei, Q.; Hu, Z.; Xu, M.; Qiu, L.; Chen, D. Redox and pH-responsive poly (amidoamine) dendrimer–poly (ethylene glycol) conjugates with disulfide linkages for efficient intracellular drug release. *Colloids Surf. B Biointerfaces* **2014**, 123, 254-263.

45. Liu, X.; Hu, D.; Jiang, Z.; Zhuang, J.; Xu, Y.; Guo, X.; Thayumanavan, S. Multi-Stimuli-Responsive Amphiphilic Assemblies through Simple Postpolymerization Modifications. *Macromolecules* **2016**, 49, 6186-6192.

46. Kono, K.; Ikeda, R.; Tsukamoto, K.; Yuba, E.; Kojima, C.; Harada, A. Polyamidoamine dendron-bearing lipids as a nonviral vector: influence of dendron generation. *Bioconjug. Chem.* **2012**, 23, 871-879.

47. Jones, S. P.; Gabrielson, N. P.; Pack, D.W.; Smith, D. K. Synergistic effects in gene delivery—a structure–activity approach to the optimisation of hybrid dendritic–lipidic transfection agents. *Chem. Commun.* **2008**, 39, 4700-4702.

48. Zhang, Y.; Chen, J.; Xiao, C.; Li, M.;Tian, H.; Chen, X. Cationic dendron-bearing lipids: investigating structure–activity relationships for small interfering RNA delivery. *Biomacromolecules* **2013**, 14, 4289-4300.

49. Dung, T. H.; Kim, J. S.; Juliano, R. L.; Yoo, H. Preparation and evaluation of cholesteryl PAMAM dendrimers as nano delivery agents for antisense oligonucleotides. *Colloids Surf. A* **2008**, 313, 273-277.

50. Schenning, A. P. H. J.; Elissen-Roman, C.; Weener, J. W.; Baars, M. W. P. L.; van der Gaast, S. J.; Meijer, E. W. Amphiphilic dendrimers as building blocks in supramolecular assemblies. *J. Am. Chem. Soc*. **1998**, 120, 8199-8208.

51. Cai, X.; Dong, C.; Dong, H.; Wang, G.; Pauletti, G. M.; Pan, X.; Wen, H.; Mehl, I.; Li, Y.; Shi, D. Effective gene delivery using stimulus-responsive catiomer designed with redox-sensitive disulfide and acid-labile imine linkers. *Biomacromolecules* **2012**,13, 1024-1034.

52. Nguyen, T. L.; Nguyen, T. H.; Nguyen, C. K.; Nguyen, D. H. Redox and pH responsive poly (amidoamine) dendrimer-heparin conjugates via disulfide linkages for letrozole delivery. *BioMed Res. Int.* **2017**: 8589212.

TABLE OF CONTENT /ABSTRACT GRAPHIC

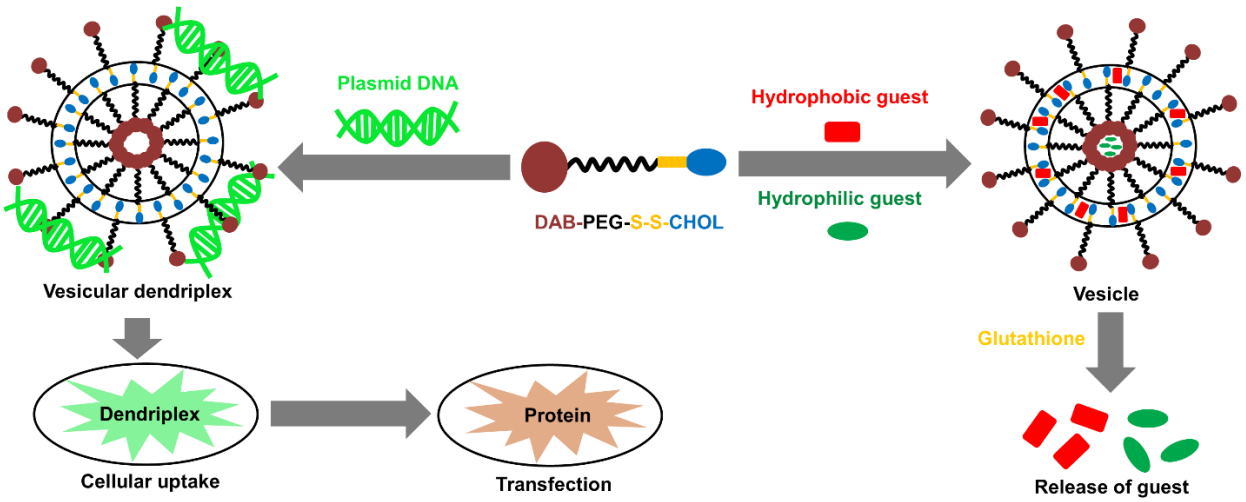

Supporting information

Redox-sensitive, cholesterol-bearing PEGylated poly(propyleneimine)-based dendrimersomes for drug and gene delivery to cancer cells

Partha Laskar,[a] Sukrut Somani,[a] Najla Altwaijry,[a] Margaret Mullin,[b] Deborah Bowering,[a,c] Monika Warzecha,[a,c] Patricia Keating, [d] Rothwelle J. Tate, [a] Hing Y. Leung,[e] and Christine Dufès,*[a]

a. Strathclyde Institute of Pharmacy and Biomedical Sciences, University of Strathclyde, 161 Cathedral Street, Glasgow G4 0RE, United Kingdom.

b. College of Medical, Veterinary and Life Sciences, University of Glasgow, Glasgow G12 8QQ, United Kingdom.

c. CMAC Future Manufacturing Research Hub, Technology and Innovation Centre, University of Strathclyde, 99 George Street, Glasgow G1 1RD, United Kingdom.

d. Department of Pure and Applied Chemistry, University of Strathclyde, 295 Cathedral Street, Glasgow G1 1XL, United Kingdom

e. Cancer Research UK Beatson Institute, Garscube Estate, Switchback Road, Bearsden, Glasgow, G61 1BD, United Kingdom.

Corresponding Author

* Corresponding author: Christine Dufès

Strathclyde Institute of Pharmacy and Biomedical Sciences, University of Strathclyde, 161 Cathedral Street, Glasgow G4 0RE, United Kingdom

Phone: 44 -141 548 3796

Fax: 44 -141 552 2562

E-mail: C.Dufes@strath.ac.uk

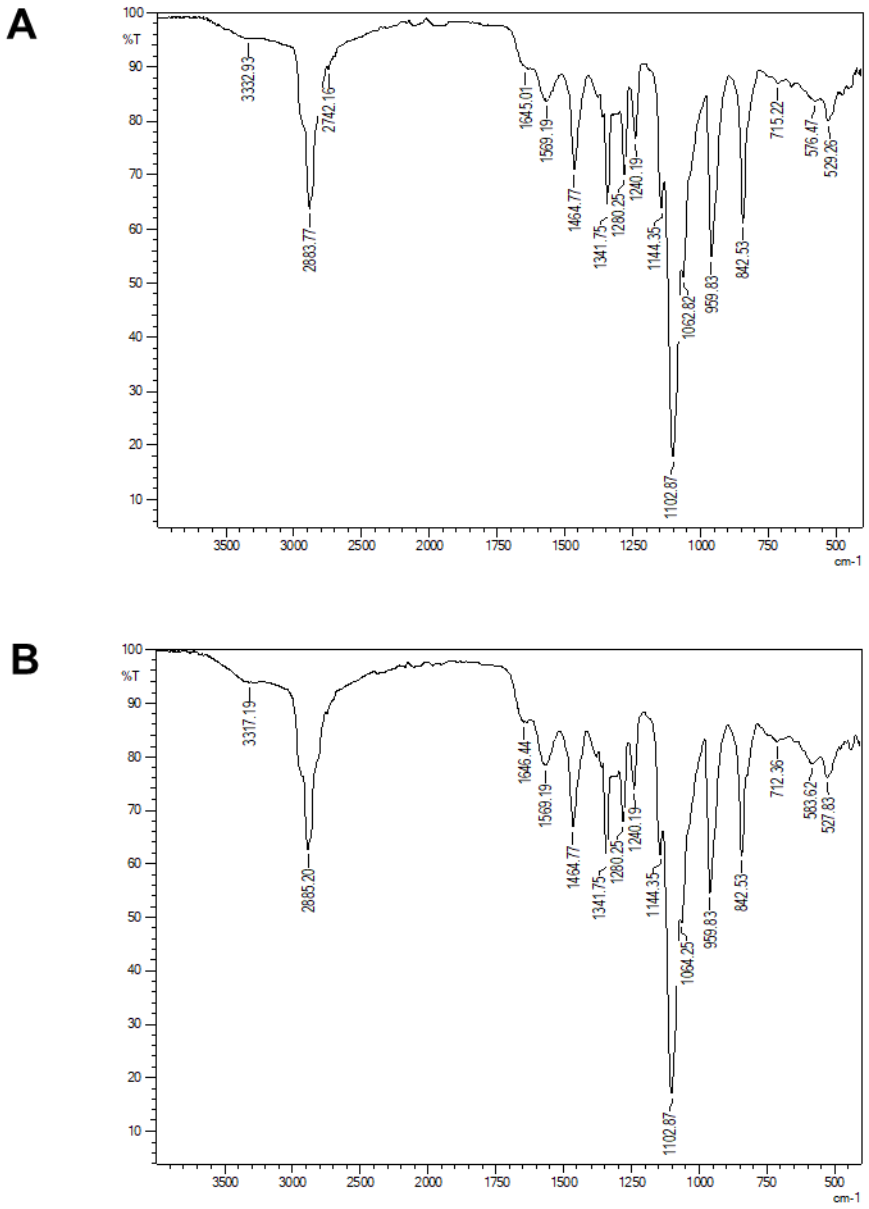

Figure S1. FTIR spectra of (A) low-cholesterol and (B) high-cholesterol dendrimers

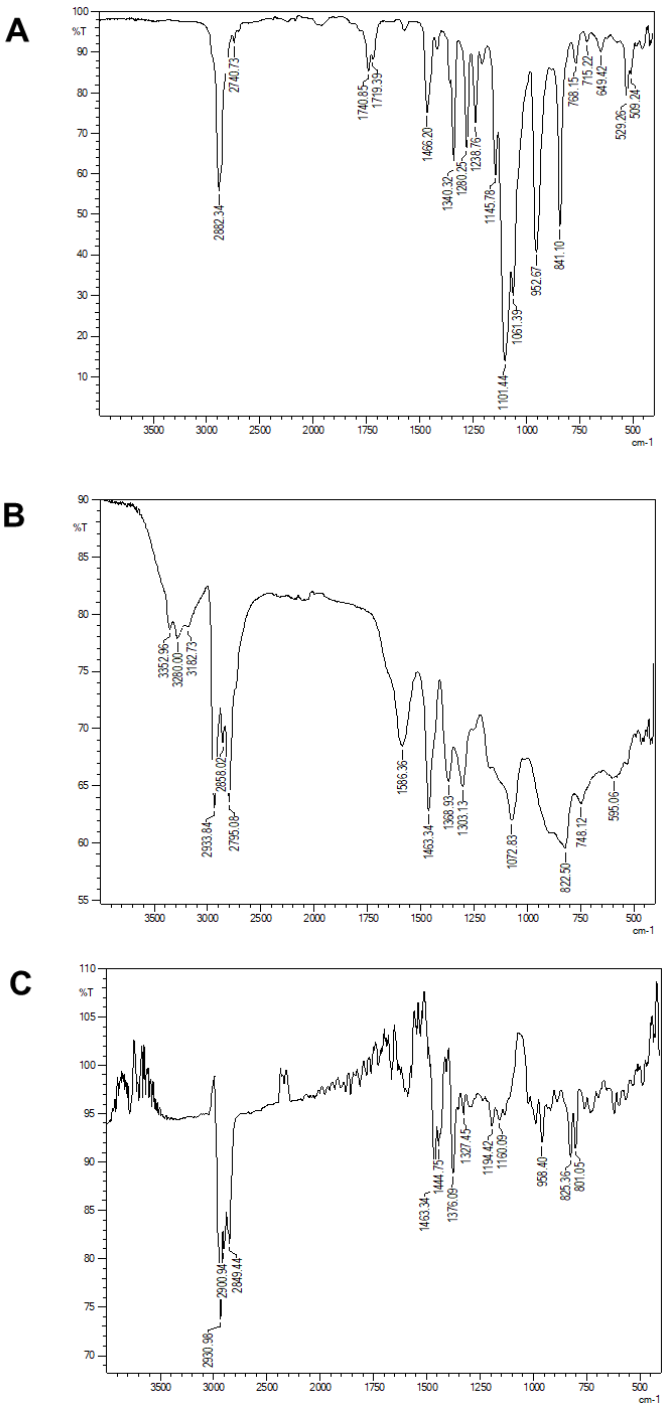

Figure S2. FTIR spectra of (A) OPSS-PEG-SCM (B) DAB dendrimer and (C) thiocholesterol

A

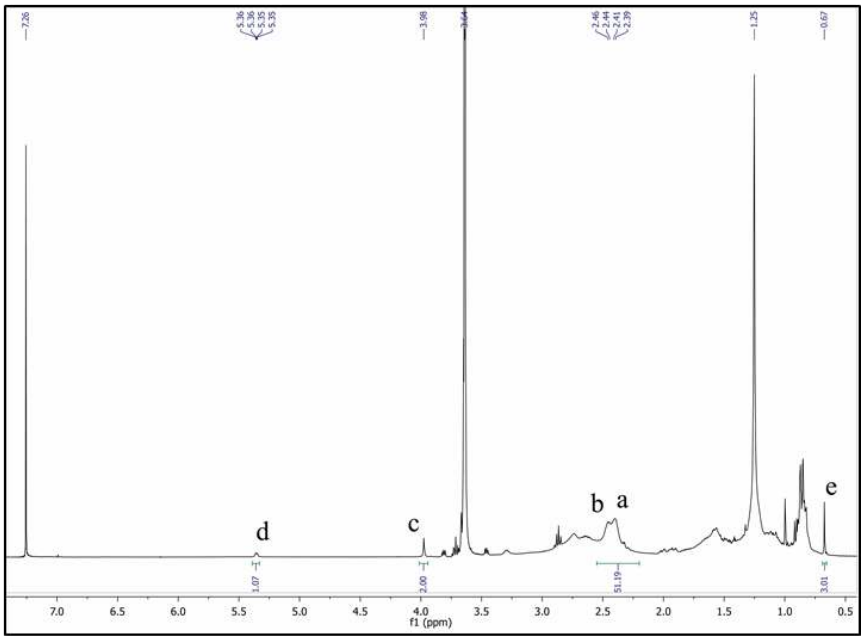

B

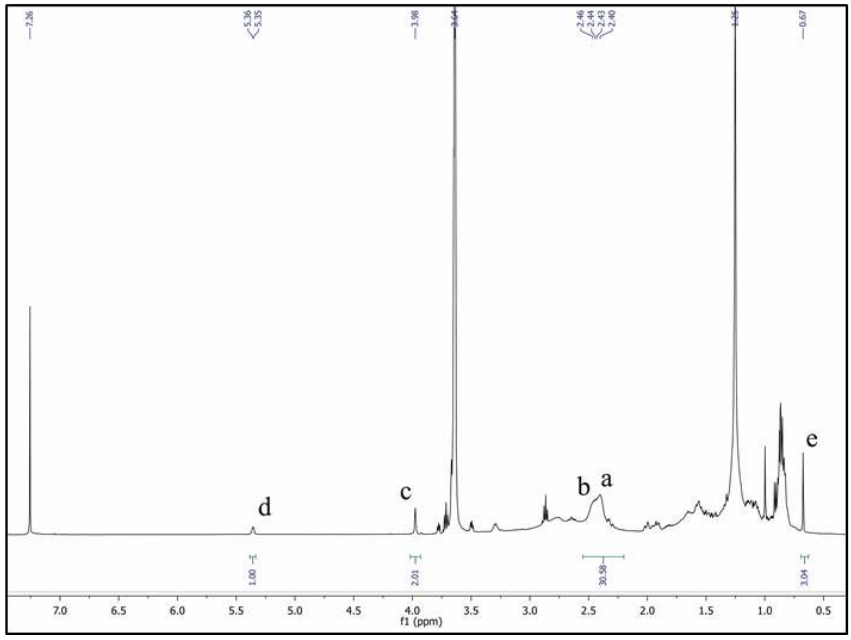

Figure S3. ^{1}H-NMR spectrum of low-cholesterol (A) and high-cholesterol (B) dendrimer (in $CDCl_3$, 500 MHz).

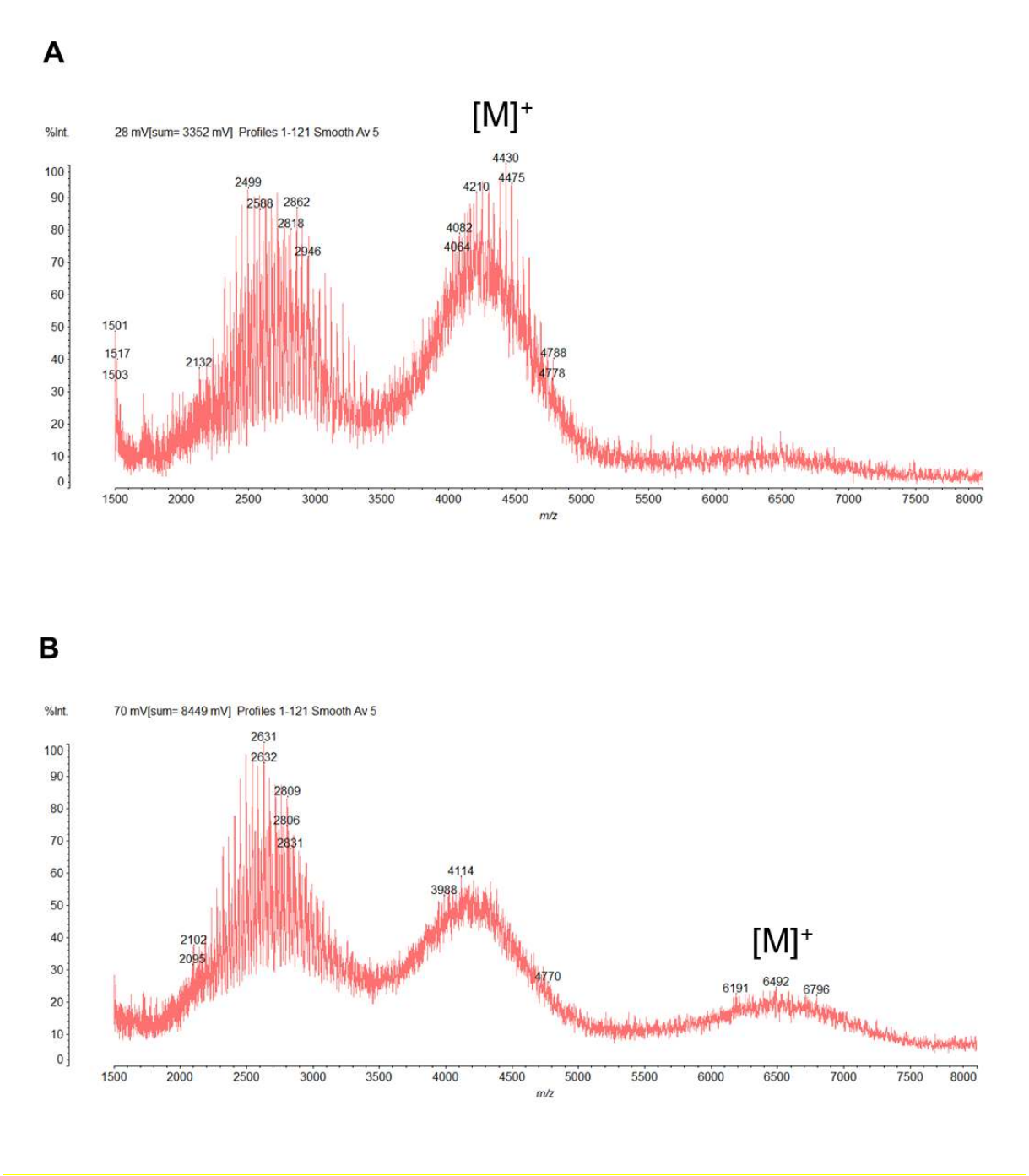

Figure S4. MALDI-TOF MS spectra of low-cholesterol (A) and high-cholesterol dendrimers (B)

Section S1. Lipid loading Calculations

The amount of lipid or cholesterol (CHOL) loading to modified dendrimer is calculated as the weight of conjugated CHOLSH as a percentage of the total average molecular weight:

Lipid-loading (%) = {(n x 401.72)/$[M]^+$}x 100

Where, n is the number of cholesterol conjugated to modified dendrimer and $[M]^+$ is the average molecular weight of the modified dendrimers analyzed from MALDI-TOF MS.

Low-cholesterol dendrimer (DPSCL), lipid loading (%) = {(1 x 401.72)/4210} x 100 = 9.54%

High-cholesterol dendrimer (DPSCH), lipid loading (%) = {(2 x 401.72)/6492} x 100 = 12.37%

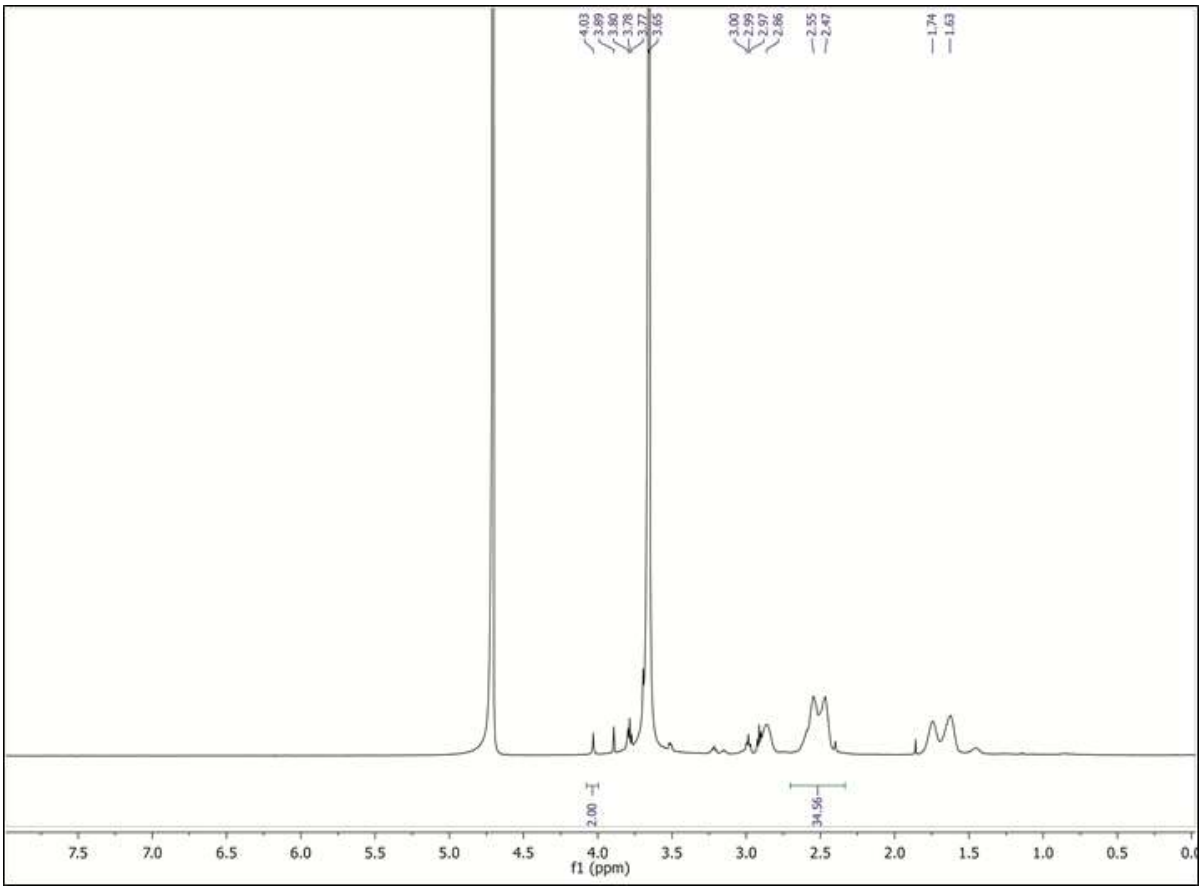

Figure S5. ^{1}H-NMR spectrum of high-cholesterol dendrimer (in D_2O, 500 MHz)

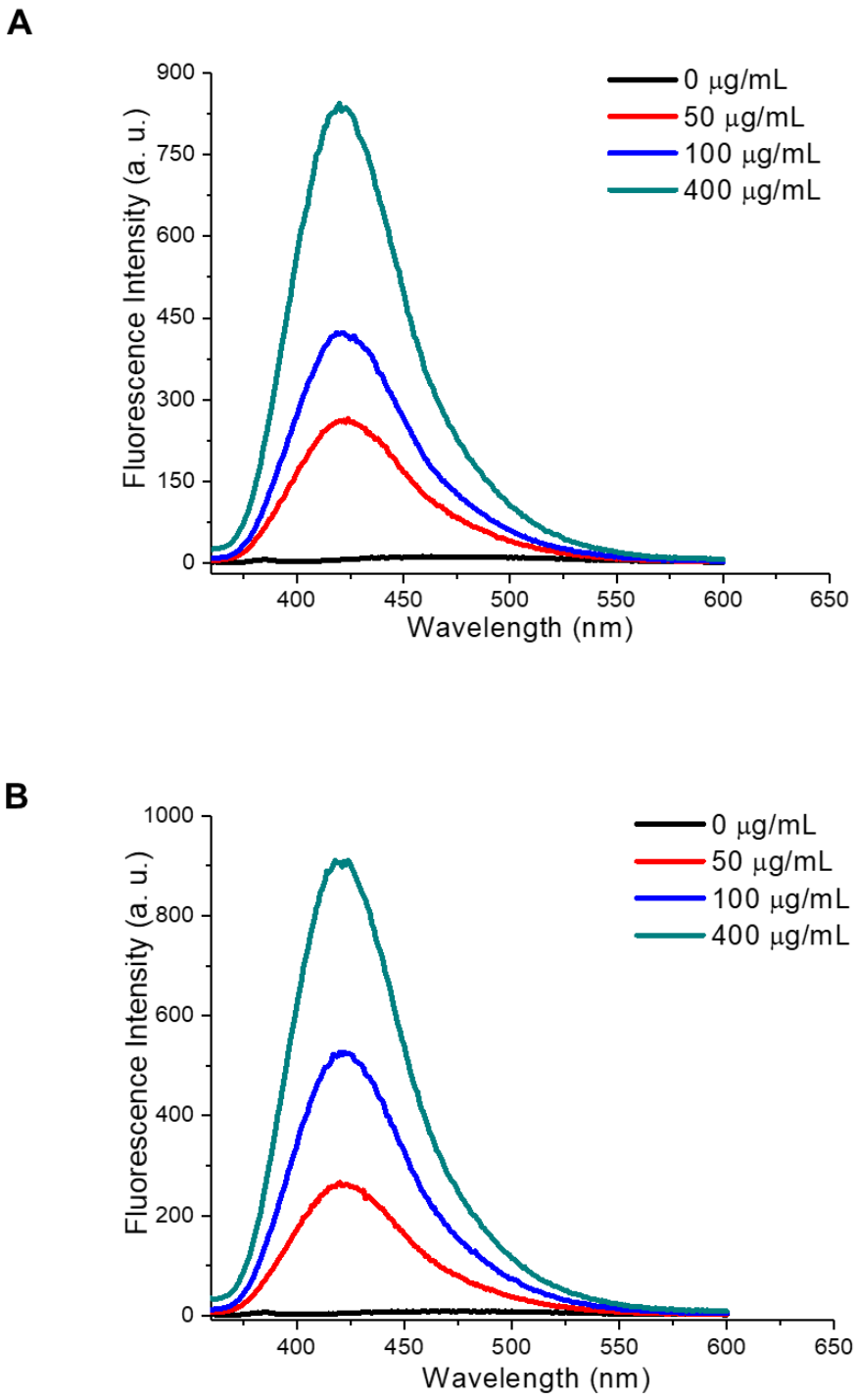

Figure S6. Fluorescence spectra of N-Phenyl-1-naphthylamine in presence or absence of low-cholesterol (A) and high-cholesterol (B) dendrimer dispersions at various concentrations in PBS buffer (pH 7.4)

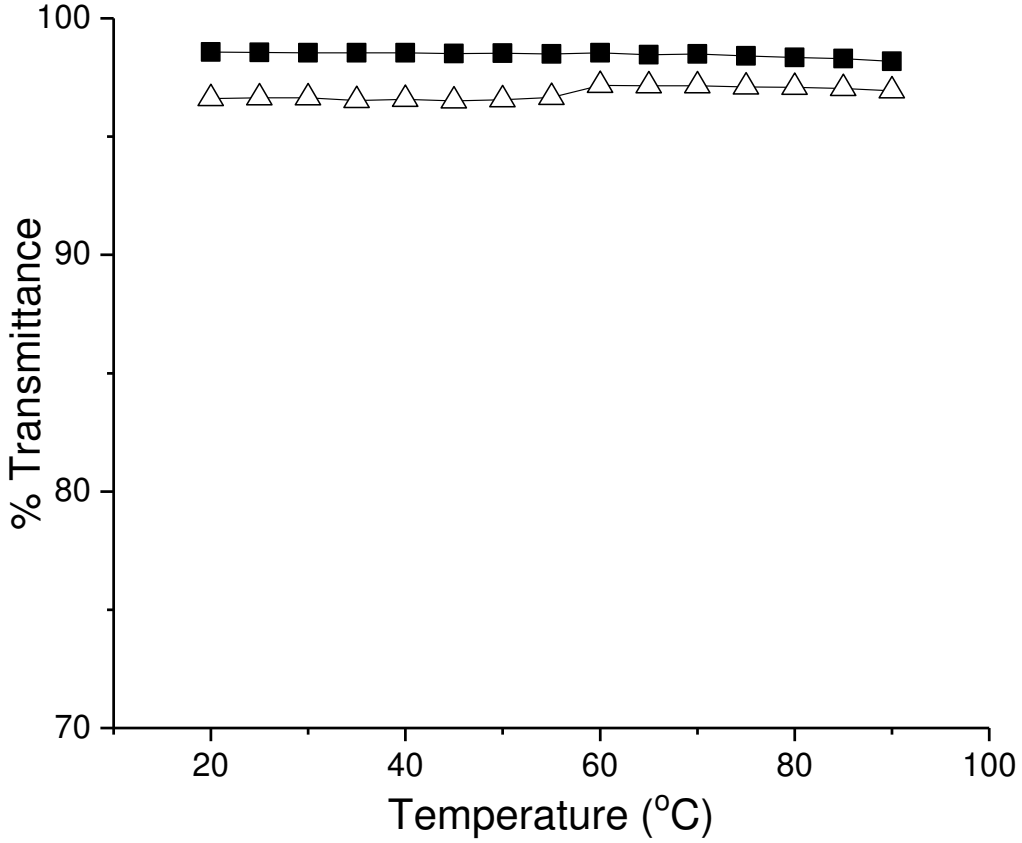

Figure S7. Transmittance of low-cholesterol (■) and high-cholesterol (○) dendrimer-based vesicles in function of temperature (400 μg/mL, pH 7.4).

Table S1. Results of phase transition analysis for low-cholesterol (DPSCL) and high-cholesterol (DPSCH) vesicles by DSC

Dendrimer	Heating cycle	Endotherm Onset T (°C)	Endotherm Peak T (°C)	Endotherm enthalpy (J/g)
DPSCL	**1st**	-0.8	0.8	-351.5
	2nd	-0.8	0.8	-343.5
DPSCH	**1st**	-0.6	-0.2	-2.03
	2nd	-0.6	-0.2	-10.26

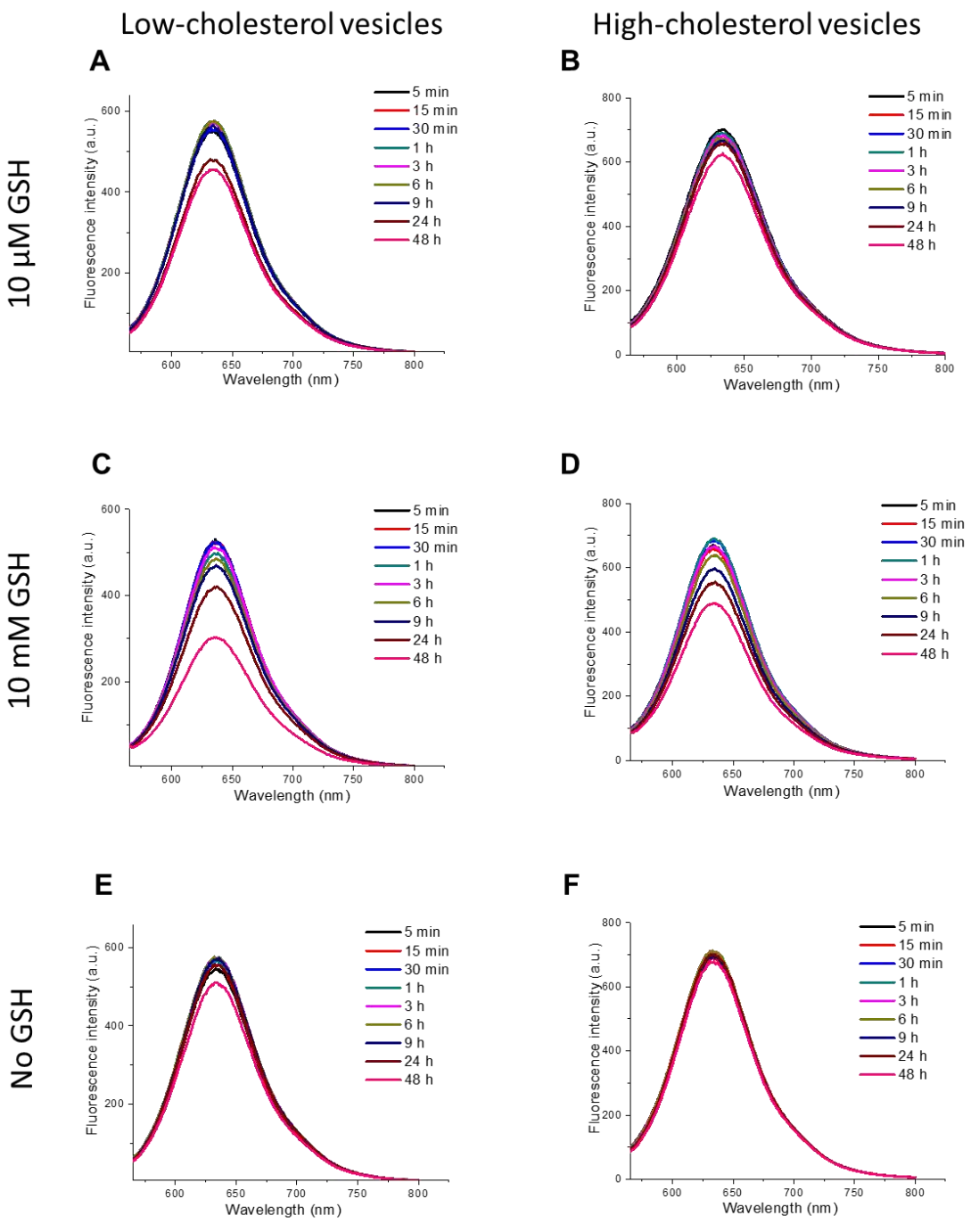

Figure S8. Fluorescence emission spectra of Nile Red entrapped in low-cholesterol (A, C, E) and high-cholesterol (B, D, F) dendrimer-based vesicles (100 µg/mL in PBS, pH 7.4) in presence of glutathione (10 µM (A, B) and 10 mM (C, D)) at various time intervals (control: no glutathione) (E, F)

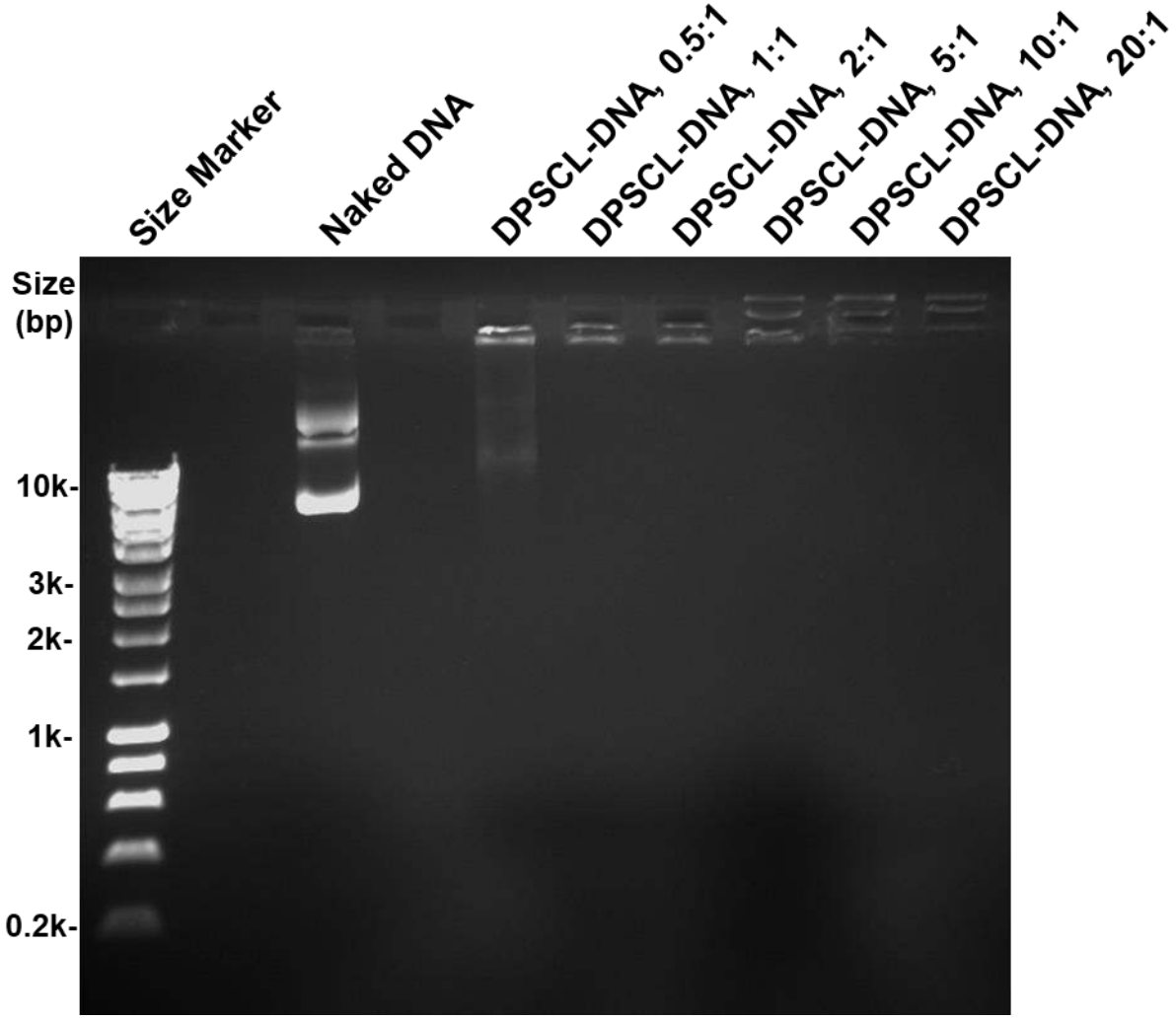

Figure S9. Gel retardation assay of low-cholesterol DAB (DPSCL) dendriplexes at various dendrimer: DNA weight ratios (0.5:1, 1:1, 2:1, 5:1, 10:1,20:1)

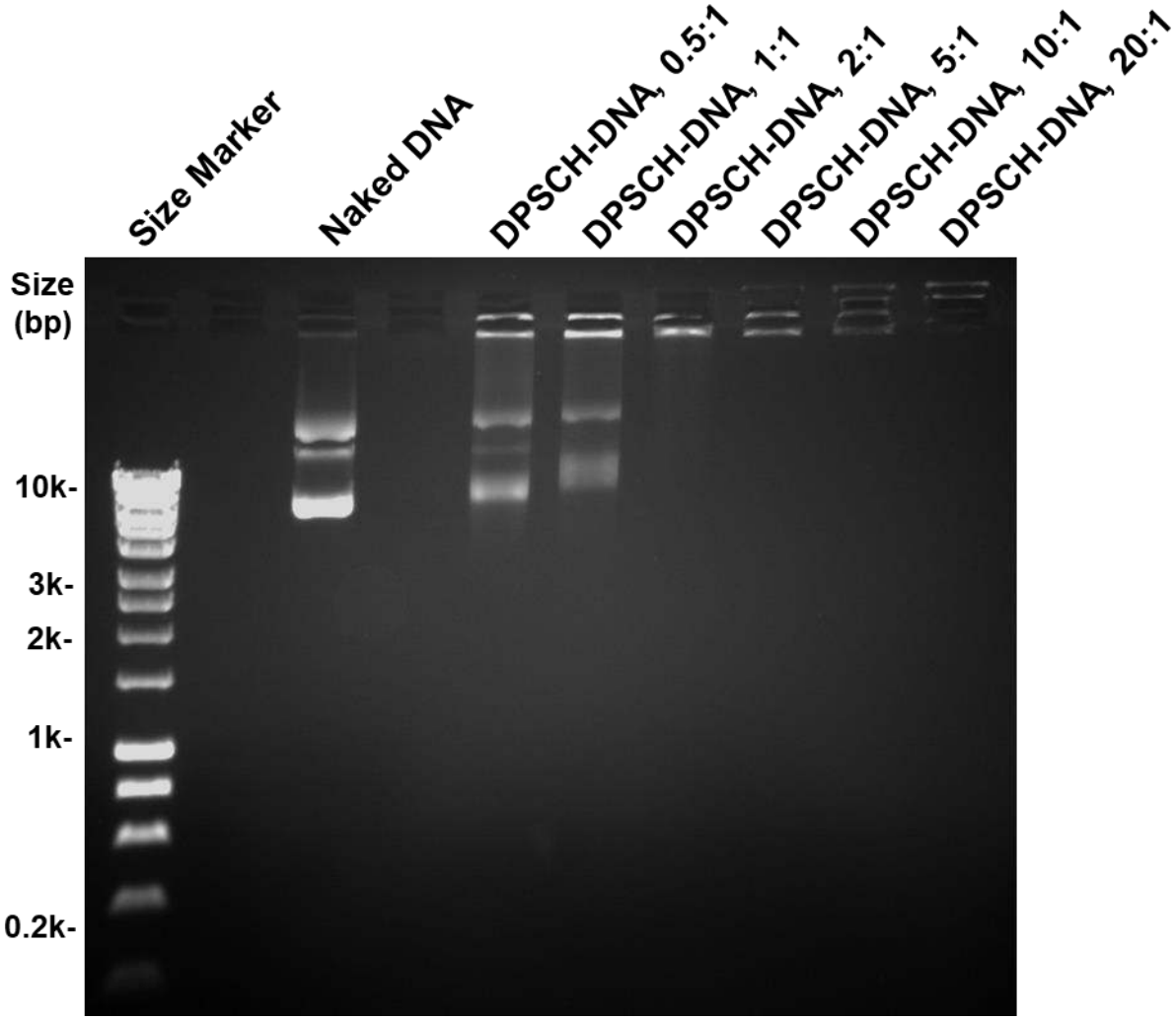

Figure S10. Gel retardation assay of high-cholesterol DAB (DPSCH) dendriplexes at various dendrimer: DNA weight ratios (0.5:1, 1:1, 2:1, 5:1, 10:1, 20:1)

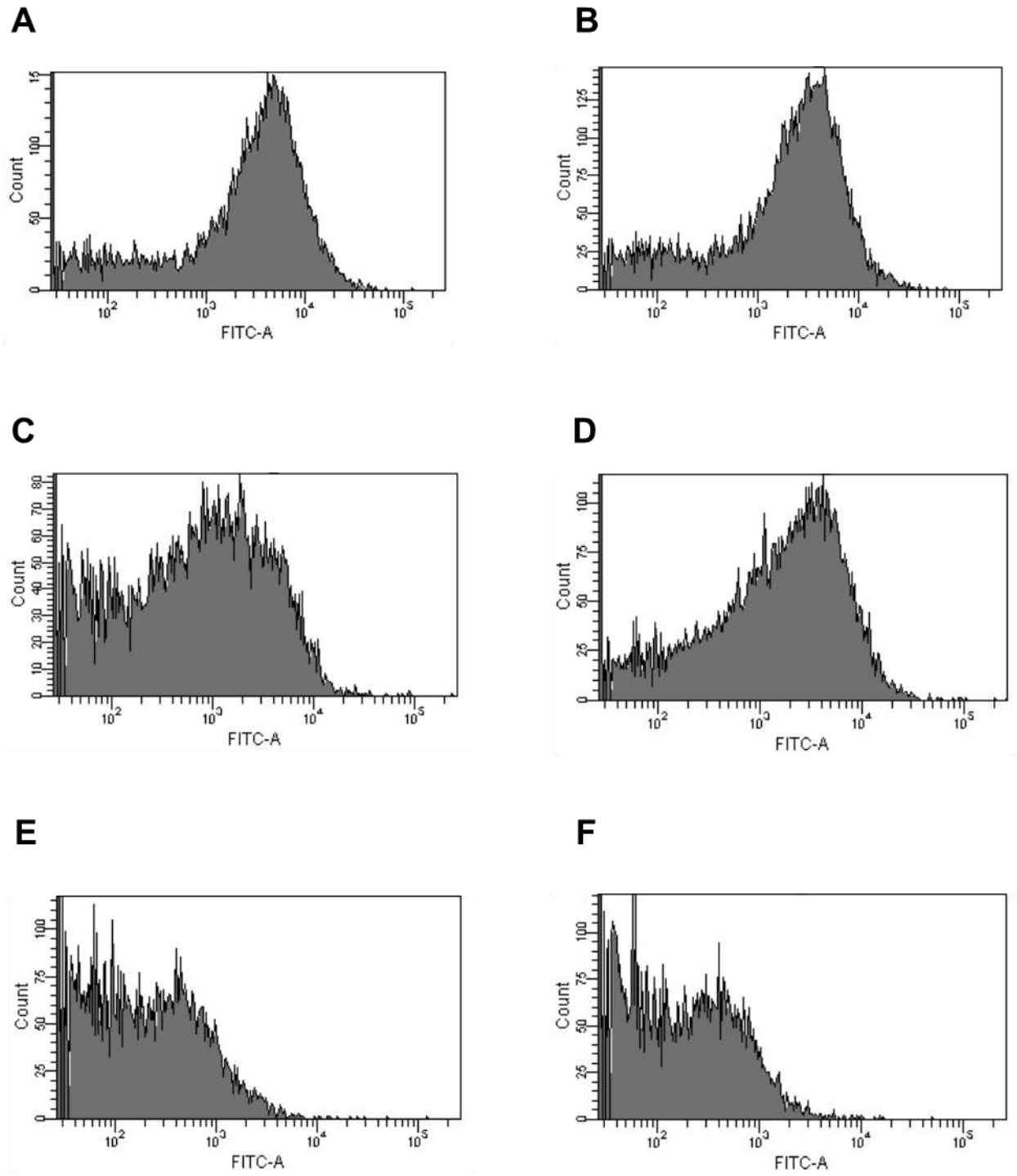

Figure S11. Flow cytometry histograms of PC3-Luc cells following 2 hours incubation with low-cholesterol dendriplex (dendrimer: DNA weight ratio 5:1 (A) or 10:1 (B)), high-cholesterol dendriplex (dendrimer: DNA weight ratio 5:1 (C) or 10:1 (D)) (Controls: DAB dendriplex (5:1) (E), DNA solution (F))